NUREG/CR-6835
ORNL/TM-2002/255

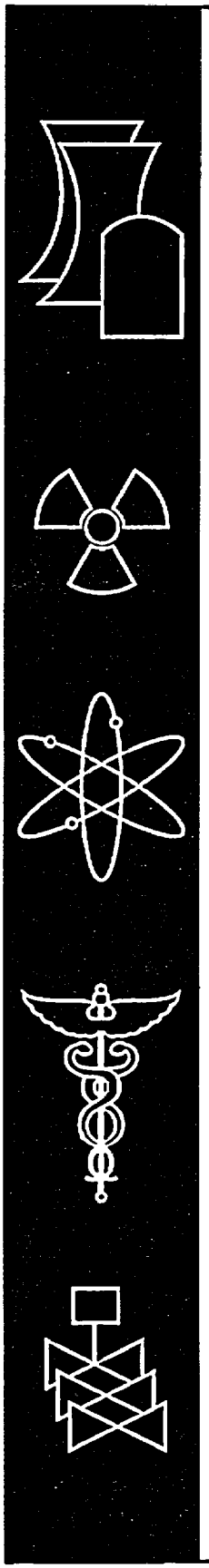

Effects of Fuel Failure on Criticality Safety and Radiation Dose for Spent Fuel Casks

Oak Ridge National Laboratory

U.S. Nuclear Regulatory Commission
Office of Nuclear Material Safety and Safeguards
Washington, DC 20555-0001

AVAILABILITY OF REFERENCE MATERIALS IN NRC PUBLICATIONS

NRC Reference Material

As of November 1999, you may electronically access NUREG-series publications and other NRC records at NRC's Public Electronic Reading Room at http://www.nrc.gov/reading-rm.html. Publicly released records include, to name a few, NUREG-series publications; *Federal Register* notices; applicant, licensee, and vendor documents and correspondence; NRC correspondence and internal memoranda; bulletins and information notices; inspection and investigative reports; licensee event reports; and Commission papers and their attachments.

NRC publications in the NUREG series, NRC regulations, and *Title 10, Energy*, in the Code of *Federal Regulations* may also be purchased from one of these two sources.

1. The Superintendent of Documents
   U.S. Government Printing Office
   Mail Stop SSOP
   Washington, DC 20402–0001
   Internet: bookstore.gpo.gov
   Telephone: 202-512-1800
   Fax: 202-512-2250
2. The National Technical Information Service
   Springfield, VA 22161–0002
   www.ntis.gov
   1–800–553–6847 or, locally, 703–605–6000

A single copy of each NRC draft report for comment is available free, to the extent of supply, upon written request as follows:

Address: Office of the Chief Information Officer,
Reproduction and Distribution
Services Section
U.S. Nuclear Regulatory Commission
Washington, DC 20555-0001
E-mail: DISTRIBUTION@nrc.gov
Facsimile: 301–415–2289

Some publications in the NUREG series that are posted at NRC's Web site address http://www.nrc.gov/reading-rm/doc-collections/nuregs are updated periodically and may differ from the last printed version. Although references to material found on a Web site bear the date the material was accessed, the material available on the date cited may subsequently be removed from the site.

Non-NRC Reference Material

Documents available from public and special technical libraries include all open literature items, such as books, journal articles, and transactions, *Federal Register* notices, Federal and State legislation, and congressional reports. Such documents as theses, dissertations, foreign reports and translations, and non-NRC conference proceedings may be purchased from their sponsoring organization.

Copies of industry codes and standards used in a substantive manner in the NRC regulatory process are maintained at—

The NRC Technical Library
Two White Flint North
11545 Rockville Pike
Rockville, MD 20852–2738

These standards are available in the library for reference use by the public. Codes and standards are usually copyrighted and may be purchased from the originating organization or, if they are American National Standards, from—

American National Standards Institute
11 West 42nd Street
New York, NY 10036–8002
www.ansi.org
212–642–4900

Legally binding regulatory requirements are stated only in laws; NRC regulations; licenses, including technical specifications; or orders, not in NUREG-series publications. The views expressed in contractor-prepared publications in this series are not necessarily those of the NRC.

The NUREG series comprises (1) technical and administrative reports and books prepared by the staff (NUREG–XXXX) or agency contractors (NUREG/CR–XXXX), (2) proceedings of conferences (NUREG/CP–XXXX), (3) reports resulting from international agreements (NUREG/IA–XXXX), (4) brochures (NUREG/BR–XXXX), and (5) compilations of legal decisions and orders of the Commission and Atomic and Safety Licensing Boards and of Directors' decisions under Section 2.206 of NRC's regulations (NUREG–0750).

NUREG/CR-6835
ORNL/TM-2002/255

Effects of Fuel Failure on Criticality Safety and Radiation Dose for Spent Fuel Casks

Manuscript Completed: August 2003
Date Published: September 2003

Prepared by
K.R. Elam, J.C. Wagner, C.V. Parks

Oak Ridge National Laboratory
Managed by UT-Battelle, LLC
Oak Ridge, TN 37831-6170

C.J. Withee, NRC Project Manager

Prepared for
Spent Fuel Project Office
Office of Nuclear Material Safety and Safeguards
U.S. Nuclear Regulatory Commission
Washington, DC 20555-0001
NRC Job Code B0009

ABSTRACT

Irradiation of nuclear fuel to high-burnup values increases the potential for fuel failure during normal and accident conditions involving transport and storage. The objective of this work is to investigate the consequences of potential fuel failure on criticality safety and external dose rates for spent nuclear fuel (SNF) storage and transport casks, with emphasis on high-burnup SNF. Analyses were performed to assess the impact of several damaged/failed fuel scenarios on the effective neutron multiplication factor (k_{eff}) and external dose rates. The damage or failure was assumed to occur during use in storage or transport, particularly in an accident. Although several of the scenarios go beyond credible conditions, they represent a theoretical limit on the effects of severe accident conditions. Further, the results provide a basis for decision making with regard to failure potential and a foundation to direct future investigations in this area.

CONTENTS

LIST OF FIGURES

LIST OF FIGURES (continued)

LIST OF FIGURES (continued)

LIST OF TABLES

ACKNOWLEDGMENTS

This work was performed under contract with the Office of Nuclear Regulatory Research, U.S. Nuclear Regulatory Commission (NRC). The authors acknowledge the review and helpful comments by Carl J. Withee, NRC Project Manager, and Oak Ridge National Laboratory colleagues Steve M. Bowman and Sedat Goluoglu.

1 INTRODUCTION

The burnup for fuel discharged from light-water reactors is continuing to increase, with target burnup values of 70 to 80 GWd/MTU desired by industry. Irradiation to these high-burnup values increases the potential for fuel failure due to the increased degradation of fuel and clad material properties with the associated intense radiation exposure. The objective of this work is to investigate the consequences of potential fuel failure on the criticality safety and external radiation dose rates for spent nuclear fuel (SNF) storage and transport casks. The consequences associated with failure of high-burnup SNF are of particular interest.

For the purposes of this study, all internal and external cask structures were assumed to remain intact, including the baskets containing the fuel assemblies and neutron poison materials. Licensing-basis assumptions were used for baseline calculations, so that comparisons of the effective neutron multiplication factor (k_{eff}) and external dose rates could be made between the baseline and the failure scenarios being evaluated. For criticality analyses, the cask was assumed to be flooded, while for dose assessment, the cask was assumed to be dry. The analyses were performed assuming uniform presence of damaged/failed fuel for several postulated scenarios, and the impact of each scenario on the relevant safety parameters (i.e., k_{eff} and external dose rates) was assessed. Although the scenarios considered go beyond credible conditions, they represent a theoretical limit on the effects of severe accident conditions.

For each cask design considered, reference fuel specifications (e.g., enrichment, burnup, and cooling time) were used. For the criticality analyses, the reference specifications were selected to correspond to k_{eff} values consistent with the recommended regulatory limit of 0.95.[1,2] For the dose assessment, the reference specifications were selected to represent high-burnup fuel, and thus the corresponding dose rates may not meet the recommended regulatory limits under normal conditions. In each case, the increase in the relevant safety parameter is of interest.

2 FUEL FAILURE SCENARIOS AFFECTING CRITICALITY SAFETY

The criticality safety analyses were performed assuming uniform presence of damaged/failed fuel for each postulated failure scenario, and the impact of each scenario on k_{eff} was assessed with respect to undamaged fuel conditions. Although not a limiting condition of the analyses, the fuel damage/failure was assumed to occur during use in storage or transport, particularly in an accident. As the radial neutron leakage from storage/transport casks is small, many of the criticality analyses were performed with three-dimensional (3-D) basket-cell models, using reflective boundary conditions to represent an infinite radial array of cask basket cells containing fuel assemblies. The applicability of these models was verified via comparison to full 3-D cask models for selected cases.

The casks and fuel assembly specifications considered are described below. Two of the casks are based on the Holtec HI-STAR 100 System[3] and are designed to accommodate fresh fuel, while the other is a conceptual cask design that relies on burnup credit for criticality safety. As fuel reactivity is sensitive to the internal cask basket structure, criticality investigations were performed with all three casks:

- Holtec HI-STAR MPC-24 cask,[3] which is licensed for storage and transport of 24 fresh pressurized-water-reactor (PWR) fuel assemblies, loaded with Westinghouse (WE) 17 × 17 fuel assemblies with an initial enrichment of 4.0 wt % ^{235}U.

- Holtec HI-STAR MPC-68 cask,[3] which is licensed for storage and transport of 68 fresh boiling-water-reactor (BWR) fuel assemblies, loaded with General Electric (GE) 8 × 8 fuel assemblies with an initial enrichment of 4.5 wt % ^{235}U. Consistent with regulatory guidance,[1,2] no burnable poisons were included in the fuel assemblies.

- GBC-32 cask,[4] which is a generic 32-PWR-assembly cask design that was developed as a burnup-credit computational benchmark. Westinghouse 17 × 17 fuel assemblies with an initial enrichment of 5.0 wt % ^{235}U, burnup values of 45 and 75 GWd/MTU, and a cooling time of 5 years were considered. Both uniform and distributed axial-burnup distributions were considered.

Potential failed fuel configurations may vary significantly, and hence there is a large degree of uncertainty in defining these configurations. For the criticality safety analyses in this section, five different fuel failure scenarios that would impact criticality safety were defined and studied. These scenarios are described below. Several of these scenarios go beyond credible conditions (e.g., the loss of fuel or structural material without any plausible explanation for where the material went and the artificial suspension of fuel pellets in water), and they merely represent a theoretical limit. The establishment of credible configurations to be used for the evaluation of a particular design must be addressed separately.

Scenario 1. ***Individual fuel rod collapse resulting in rods being absent from the assembly lattice.*** This is significant because fuel assemblies are designed to be undermoderated, and the loss of fuel pins from the lattice results in increased moderation, which can increase k_{eff}.

Scenario 2. ***Loss of fuel rod cladding.*** The loss of cladding provides space for more water around the fuel pins, which increases moderation of the lattice and subsequently increases k_{eff}.

Scenario 3. ***Collapse of fuel rods to form zones of optimum-moderated fuel pellets.*** Collapse of fuel rods and disintegration of fuel hardware and cladding are assumed to leave each cask basket full of fuel pellets (cylinders) at optimum spacing.

Scenario 4. ***Axial regions with no neutron poison in the basket.*** Loss of the assembly hardware and/or spacer allows the fuel assemblies to slip into an axial region with no neutron poison coverage in the basket.

Scenario 5. ***Variation in fuel rod (without cladding) pitch.*** Fuel rods without cladding are allowed to increase in pitch in a regular lattice within the basket cell until either the optimum pitch is reached or the outer rods reach the cell walls. If the latter occurs, rows of fuel rods are removed from the lattice and the pitch is allowed to increase further. The intention is to find the maximum k_{eff} associated with such variations.

2.1 DESCRIPTION OF CASK MODELS

Using KENO V.a, a part of the SCALE computer code system,[5] 3-D full-cask and basket-cell models were developed to perform criticality safety calculations for scenarios 1, 2, 4, and 5. A KENO-VI model of each cask basket cell was used for scenario 3 to use the dodecahedron and dodecahedral array geometry capability of this code. In each model, full water flooding was assumed, including water in the gap between the fuel pellets and cladding (where cladding is assumed to be present). The important dimensions associated with both full-cask and basket-cell models of each cask are given in Table 1.

The basket-cell models are reflected to form an infinite radial array of fuel baskets. With the exception of scenario 4, the cask top and bottom are not included in the basket-cell models. The model used for scenario 4 includes the cask baseplate, since it becomes neutronically important as the fuel assembly is allowed to slip downward. Also, the walls in the basket-cell model for scenario 4 extend to the floor of the cask, which is modeled as 30 cm below the bottom of the fuel. However, the Boral plates remain aligned axially with the original location of the active fuel and were assumed to be the same length as the active fuel region.

Table 1 Cask and basket-cell dimensions

Dimension	MPC-24	GBC-32	MPC-68
Active fuel length (cm)	365.76	365.76	381.0
Cask wall, steel thickness (cm)	21.86	20.0	15.24
Cask baseplate, steel thickness (cm)	21.59	30.0	21.59
Cask top, steel thickness (cm)	39.37	20.0	39.37
Water below active fuel (cm)	10.16	30.0	18.542
Water above active fuel (cm)	15.24	30.0	21.488
Basket wall, steel thickness (cm)	0.7938	0.75	0.635
Basket pitch (cm)	27.374	23.7565	16.332
Boron loading (^{10}B g/cm^2)	0.02	0.0225	0.0279

The atom densities for the fuel used in each of the three cask models are given in Table 2. Compositional data for fuel in the GBC-32 cask were calculated with the SAS2H sequence of SCALE for uniform burnup values of 45 and 75 GWd/MTU and a cooling time of 5 years.

Table 2 Atom densities for fuel

Nuclide	MPC-24	GBC-32 (45 GWd/MTU)	GBC-32 (75 GWd/MTU)	MPC-68
O-16	4.693E–02	4.69E–02	4.69E–02	4.693E–02
U-235	9.505E–04	3.17E–04	9.65E–05	1.023E–03
U-238	2.252E–02	2.07E–02	2.02E–02	2.246E–02
U-234		5.85E–06	4.10E–06	
U-236		1.48E–04	1.64E–04	
Np-237		1.59E–05	2.63E–05	
Pu-238		5.58E–06	1.58E–05	
Pu-239		1.49E–04	1.48E–04	
Pu-240		5.71E–05	7.99E–05	
Pu-241		2.91E–05	3.84E–05	
Pu-242		1.35E–05	3.62E–05	
Am-241		8.72E–06	1.16E–05	
Am-243		3.13E–06	1.26E–05	

2.1.1 MPC-24 Cask Model

The MPC-24 cask model is based on the Holtec HI-STAR 100 system with the MPC-24 canister.[3] For this analysis, the cask was loaded with fresh PWR assemblies enriched to 4.0 wt % ^{235}U. The fuel assemblies are based on WE 17 × 17 fuel assemblies but have all of the top and bottom end fittings, grid spacers, and other hardware removed. Each assembly has 264 fuel pins and 25 guide/instrument tubes, which are modeled as zirconium cylinders filled with water.

Figure 1 shows a slice of the MPC-24 basket-cell model, including the cell walls, Boral panels, and a thickness of water to provide the proper basket pitch when the model is reflected radially. The fuel baskets into which the assemblies are placed are made of stainless steel and are 365.76 cm in length to match the active fuel length. Boral panels are attached on the outside of each basket-cell wall and are also modeled the same length as the active fuel. A water gap is present between basket cells, forming a flux trap for thermal neutrons. The boron loading in each Boral panel is 0.02 g $^{10}B/cm^2$.

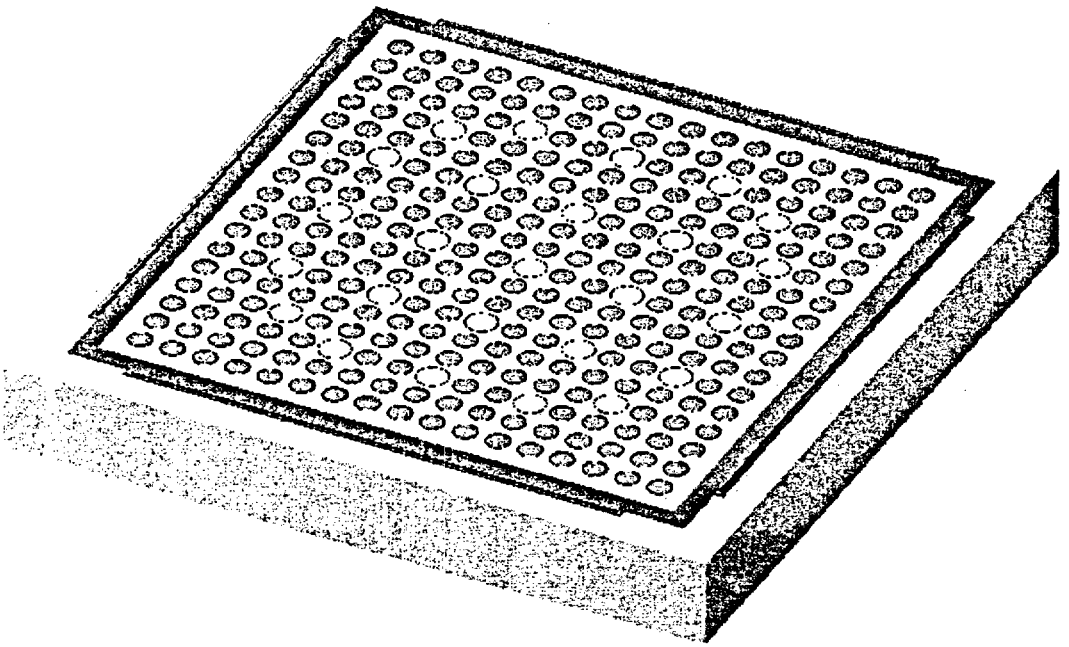

Figure 1 MPC-24 basket-cell model

2.1.2 GBC-32 Cask Model

The GBC-32 cask model is based on a generic high-capacity PWR fuel assembly cask originally designed as a computational benchmark for burnup-credit calculations, as described in Ref. 4. This cask is included to allow a comparison of consequences between high-burnup fuel and fresh fuel. As shown in Table 2, the fuel compositions used for the criticality calculations include only the actinides used in Ref. 4 and do not include fission products.

As with the MPC-24 model, the fuel assemblies in the GBC-32 cask are based on WE 17 × 17 fuel assemblies and are modeled without the top and bottom end fittings, grid spacers, and other hardware. Cases with both uniform axial burnup and distributed axial burnup based on the representative axial profile in Ref. 4 were considered. Each assembly has 264 fuel pins and 25 guide/instrument tubes, which are modeled as zirconium cylinders filled with water.

The basket cells into which the assemblies are placed are made of stainless steel and are 365.76 cm in length to match the active fuel length. Boral panels are attached between each cell and are also the same length as the active fuel. The boron loading in each panel is 0.0225 g $^{10}B/cm^2$. Unlike the MPC-24 cask, there is no water gap between the basket cells.

Figure 2 shows a slice of the GBC-32 basket-cell model, including the basket walls and one-half thickness of the Boral panels. Reflecting this cell model on all four sides provides a full thickness of Boral between fuel assemblies.

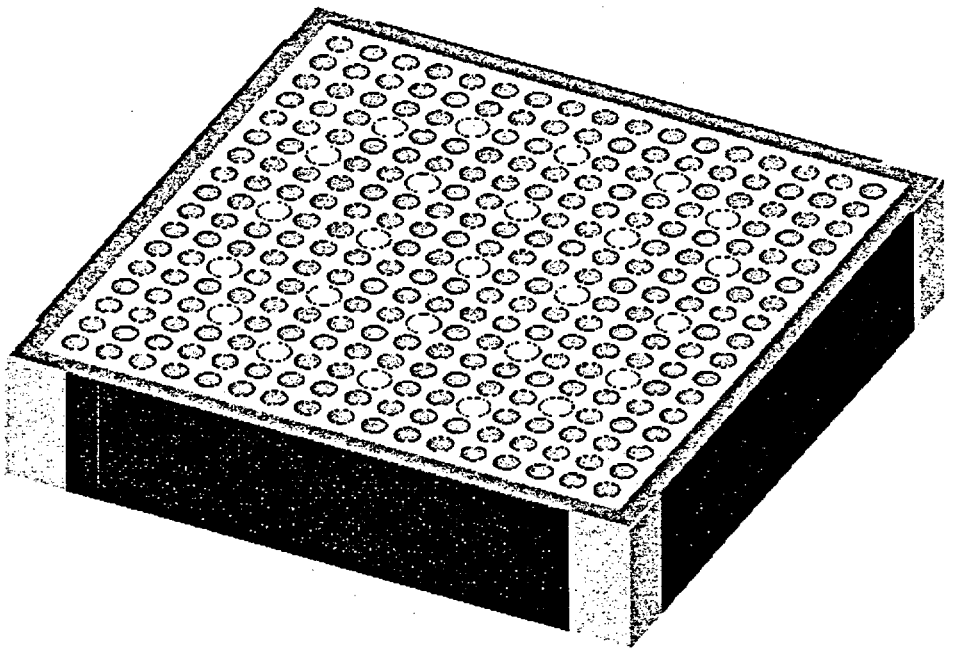

Figure 2 GBC-32 basket-cell model

2.1.3 MPC-68 Cask Model

The MPC-68 cask model is based on the Holtec HI-STAR 100 system with the MPC-68 canister.[3] For this analysis, the cask was loaded with BWR assemblies enriched to 4.5 wt % ^{235}U with no burnable-poison material. The fuel assemblies are based on GE 8 × 8 fuel assemblies but have all of the top and bottom end fittings, grid spacers, and other hardware removed. Each assembly has 62 fuel pins and 2 water holes, which are modeled as zirconium cylinders filled with water. The assemblies are inside zirconium channels, which are 0.254 cm thick and are 381.0 cm in length to match the fuel pins.

The fuel baskets are made of stainless steel and are 381.0 cm in length to match the active fuel length. Boral panels are attached on the inside of two faces of each fuel basket and are also the same length as the active fuel. The boron loading in each panel is 0.0279 g $^{10}B/cm^2$.

Figure 3 shows a slice of the MPC-68 basket-cell model, including the basket walls, Boral panels, and a thickness of water to provide a basket pitch of 16.332 cm. Periodic reflection of this cell model on all four sides provides a full thickness of Boral between fuel assemblies.

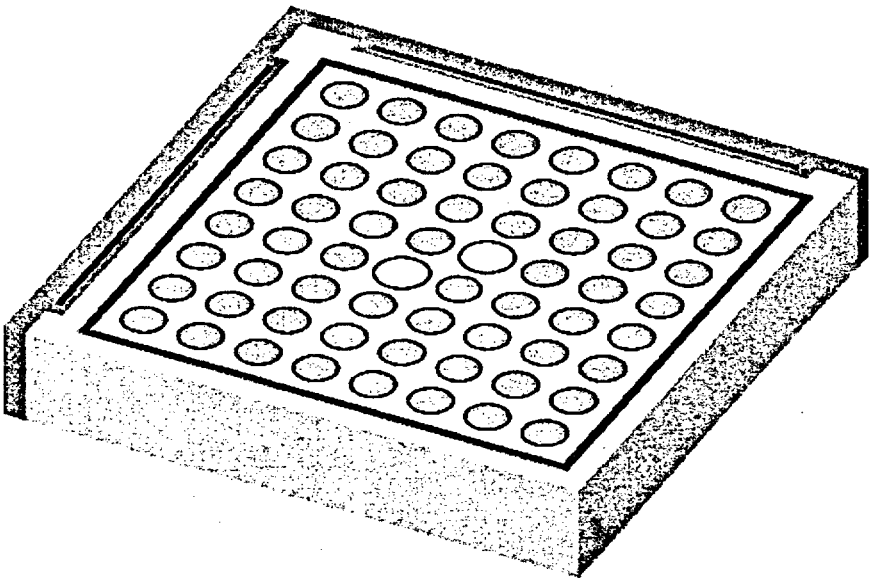

Figure 3 MPC-68 basket-cell model

2.2 ANALYSIS

Each fuel failure scenario was evaluated with respect to baseline full-cask and basket-cell models with intact (unchanged) fuel by comparing the calculated values of k_{eff}. The baseline k_{eff} values are given in Table 3. The Monte Carlo standard deviation of each calculated value is approximately 0.0004.

Table 3 Baseline calculated k_{eff} values with intact (undamaged) fuel

Cask	Full-cask model	Basket-cell model
MPC-24	0.9369	0.9682
GBC-32 (uniform axial burnup of 45 GWd/MTU)	0.9623	0.9927
GBC-32 (axially distributed burnup of 45 GWd/MTU)	0.9847	1.0141
GBC-32 (uniform axial burnup of 75 GWd/MTU)	0.8253	0.8519
GBC-32 (axially distributed burnup of 75 GWd/MTU)	0.8869	0.9134
MPC-68	0.9358	0.9631

2.2.1 Individual Fuel Rod Collapse

2.2.1.1 Loss of a single fuel rod

This scenario involves fuel failure in which an individual fuel rod collapses, resulting in the removal of that rod from the assembly lattice. As discussed in Section 1, this is significant because fuel assemblies are designed to be undermoderated, and the loss of a fuel pin from the lattice causes a local area of higher moderation, which can increase k_{eff}. To conduct the analysis, each rod in a basket-cell model was removed one at a time to quantify its effect on k_{eff}. Near the center of the assembly lattice, the removal of a rod increases the moderation level for adjacent rods and results in an increase in k_{eff}. Closer to the edge of the assembly, the removal of a rod increases moderation near the thermal neutron poison panels and, in many cases, decreases k_{eff}.

For the WE 17 × 17 assembly, which was used in both the MPC-24 and GBC-32 cask models, the impact on k_{eff} of removing a single rod was very small and within the statistical uncertainty of the Monte Carlo calculations, which is less than 0.0005 in all cases. Therefore, an individual calculation was performed for each rod and the 1/8th assembly symmetry was used to average the results and reduce the effect of the statistical uncertainties. As a result, diagonal and central row/column position results are based on the average of four calculations, while the remaining position results are based on the average of eight calculations. The Δk values resulting from single rod removal in the MPC-24 basket-cell model range from –0.0009 for rods near the edge of the lattice to +0.0013 for rods near the center. Figure 4 shows the change in k_{eff} for removal of each fuel rod in one quadrant of the 17 × 17 assembly. Spaces containing a guide tube were evaluated by replacing the guide tube with water.

For the GBC-32 cask, the change in k_{eff} due to the removal of each rod was calculated for burnup values of 45 and 75 GWd/MTU. Further, separate cases considered both uniform and axially distributed burnup, resulting in the following four different fuel conditions: (1) 45 GWd/MTU, assuming uniform axial burnup; (2) 45 GWd/MTU, assuming axially distributed burnup; (3) 75 GWd/MTU, assuming uniform axial burnup; and (4) 75 GWd/MTU, assuming axially distributed burnup. Figures 5 through 8 show the change in k_{eff} associated with the removal of each fuel rod (in one quadrant of the 17 × 17 assembly) for the four different fuel conditions. For the cases with uniform axial burnup, the change in k_{eff} associated with the removal of each fuel rod becomes less positive with increasing burnup, while the opposite behavior is observed when the distributed axial burnup is included. However, in all cases, the effect of each rod on k_{eff} is less than +0.001.

Despite half-cell symmetry across the diagonal, a separate calculation was performed for each rod in the MPC-68 basket-cell model. The Δk values resulting from single rod removal range from –0.0079 for rods near the edge of the lattice to +0.0036 for rods near the center. Because of the fewer number of rods in the 8 × 8 assembly, the impact on k_{eff} of removing a single rod is notably larger than that observed with the 17 × 17 assembly in the PWR casks. Hence, the statistical uncertainties were less of a concern for the MPC-68 cases, and each Δk value is based on a single calculation with statistical uncertainty less than 0.0005. Figure 9 shows the change in k_{eff} for removal of each rod in the 8 × 8 fuel assembly. Spaces containing a water hole were evaluated by replacing the zirconium tube with water.

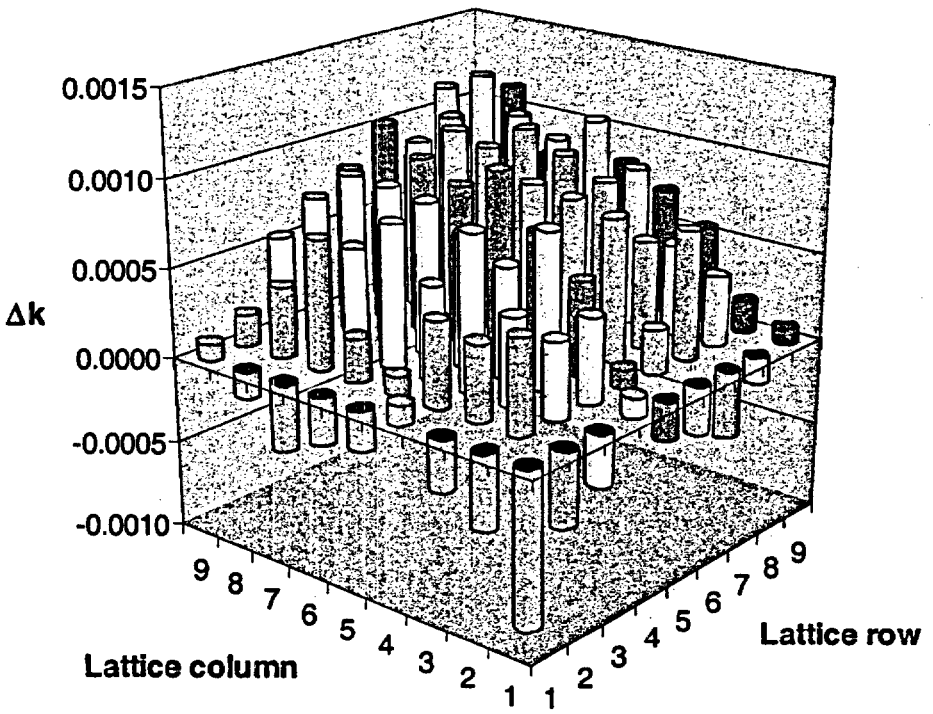

Column/row	1	2	3	4	5	6	7	8	9
1	–0.0009	–0.0004	–0.0003	0.0001	–0.0002	–0.0003	–0.0004	–0.0002	0.0001
2	–0.0004	0.0005	0.0004	0.0005	0.0001	0.0003	0.0007	0.0004	0.0002
3	–0.0003	0.0004	0.0005	0.0009	0.0005	0.0008	0.0006	0.0005	0.0006
4	0.0001	0.0005	0.0009	0.0006	0.0007	0.0009	0.0009	0.0009	0.0007
5	–0.0002	0.0001	0.0005	0.0007	0.0010	0.0009	0.0010	0.0011	0.0008
6	–0.0003	0.0003	0.0008	0.0009	0.0009	0.0003	0.0011	0.0010	0.0005
7	–0.0004	0.0007	0.0006	0.0009	0.0010	0.0011	0.0009	0.0011	0.0008
8	–0.0002	0.0004	0.0005	0.0009	0.0011	0.0010	0.0011	0.0013	0.0011
9	0.0001	0.0002	0.0006	0.0007	0.0008	0.0005	0.0008	0.0011	0.0005

Figure 4 Change in k_{eff} for single rod removal in the MPC-24 basket cell for one quadrant of the 17 × 17 fuel assembly. The tabulated values are shown beneath the graphical representation.

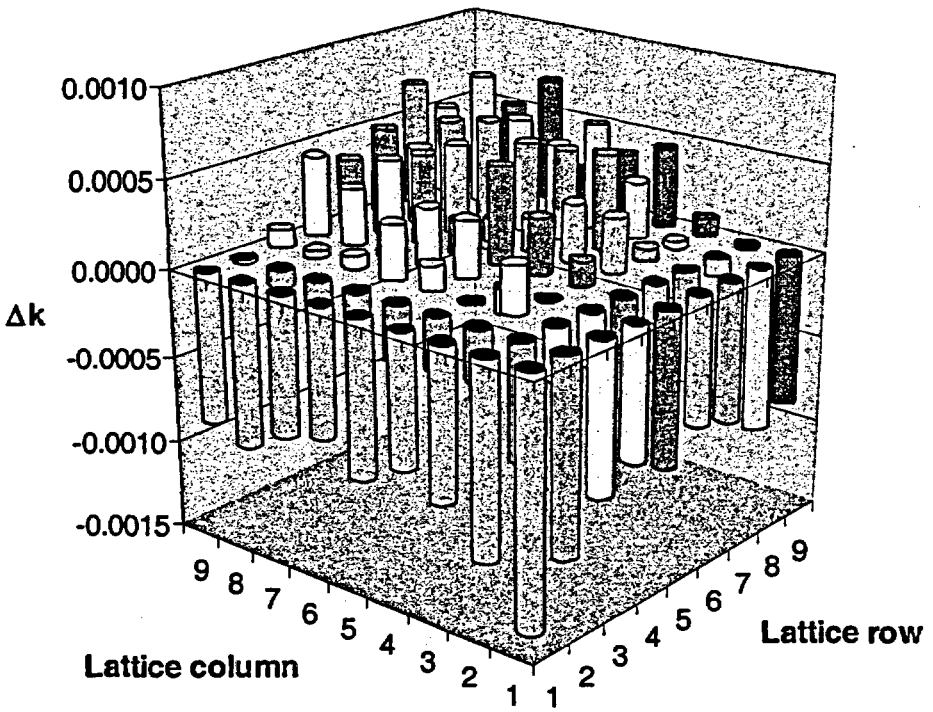

Column/row	1	2	3	4	5	6	7	8	9
1	–0.0014	–0.0011	–0.0009	–0.0008	–0.0009	–0.0007	–0.0008	–0.0009	–0.0009
2	–0.0011	–0.0007	–0.0003	–0.0003	–0.0003	–0.0002	–0.0002	–0.0001	0.0000
3	–0.0009	–0.0003	0.0003	0.0000	0.0001	0.0003	0.0001	0.0000	0.0001
4	–0.0008	–0.0003	0.0000	–0.0001	0.0003	0.0003	0.0005	0.0003	0.0005
5	–0.0009	–0.0003	0.0001	0.0003	0.0006	0.0002	0.0005	0.0006	0.0004
6	–0.0007	–0.0002	0.0003	0.0003	0.0002	0.0001	0.0005	0.0004	0.0002
7	–0.0008	–0.0002	0.0001	0.0005	0.0005	0.0005	0.0006	0.0005	0.0007
8	–0.0009	–0.0001	0.0000	0.0003	0.0006	0.0004	0.0005	0.0007	0.0005
9	–0.0009	0.0000	0.0001	0.0005	0.0004	0.0002	0.0007	0.0005	0.0002

Figure 5 Change in k_{eff} for single rod removal in the GBC-32 basket cell for one quadrant of the 17 × 17 fuel assembly with uniform axial burnup of 45 GWd/MTU. The tabulated values are shown beneath the graphical representation.

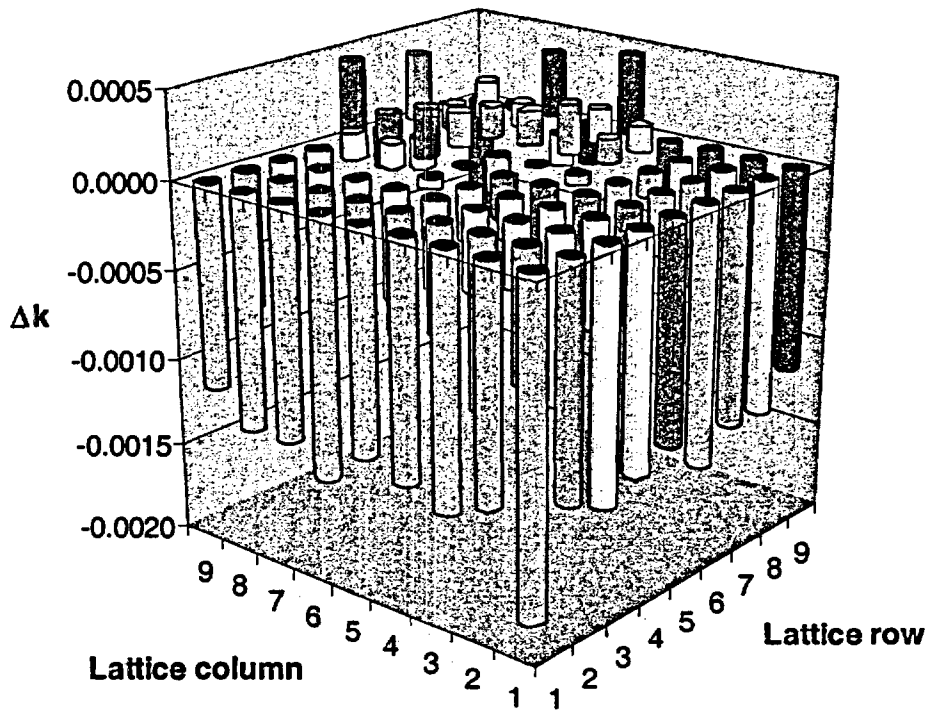

Column/row	1	2	3	4	5	6	7	8	9
1	–0.0018	–0.0013	–0.0014	–0.0013	–0.0013	–0.0015	–0.0013	–0.0013	–0.0012
2	–0.0013	–0.0007	–0.0009	–0.0006	–0.0006	–0.0003	–0.0006	–0.0005	–0.0008
3	–0.0014	–0.0009	–0.0004	–0.0005	–0.0005	–0.0006	–0.0001	–0.0003	–0.0006
4	–0.0013	–0.0006	–0.0005	–0.0002	–0.0003	–0.0001	0.0001	0.0002	–0.0003
5	–0.0013	–0.0006	–0.0005	–0.0003	–0.0002	0.0000	0.0003	0.0002	0.0005
6	–0.0015	–0.0003	–0.0006	–0.0001	0.0000	–0.0002	0.0002	–0.0002	–0.0002
7	–0.0013	–0.0006	–0.0001	0.0001	0.0003	0.0002	0.0002	0.0001	0.0004
8	–0.0013	–0.0005	–0.0003	0.0002	0.0002	–0.0002	0.0001	0.0002	0.0000
9	–0.0012	–0.0008	–0.0006	–0.0003	0.0005	–0.0002	0.0004	0.0000	–0.0006

Figure 6 Change in k_{eff} for single rod removal in the GBC-32 basket cell for one quadrant of the 17 × 17 fuel assembly with axially distributed burnup of 45 GWd/MTU. The tabulated values are shown beneath the graphical representation.

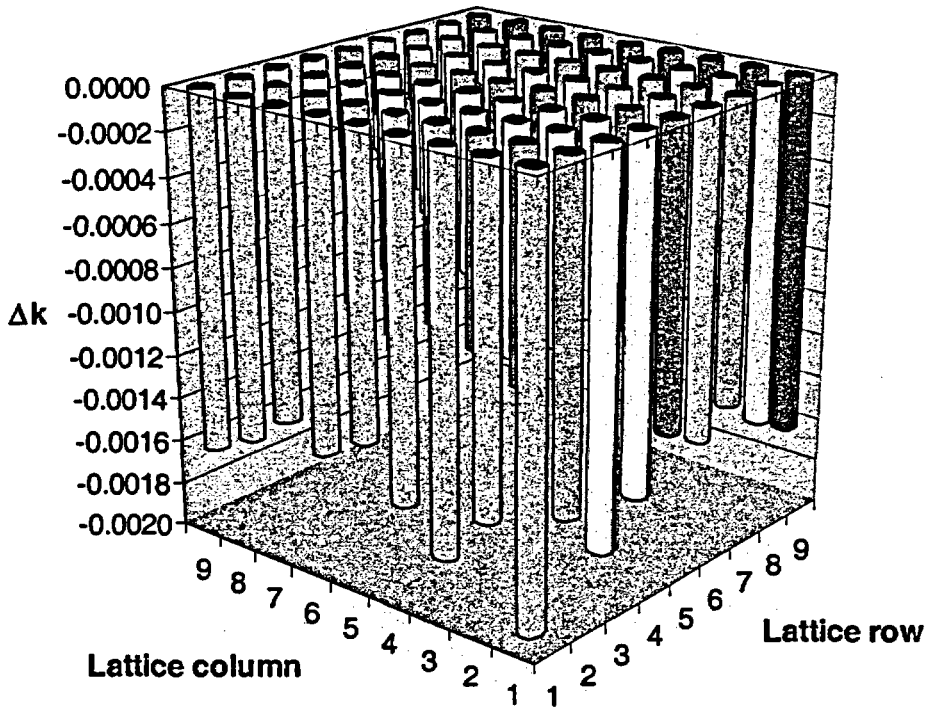

Column/row	1	2	3	4	5	6	7	8	9
1	–0.0019	–0.0015	–0.0017	–0.0016	–0.0014	–0.0015	–0.0014	–0.0015	–0.0016
2	–0.0015	–0.0010	–0.0009	–0.0008	–0.0009	–0.0009	–0.0009	–0.0012	–0.0010
3	–0.0017	–0.0009	–0.0010	–0.0007	–0.0005	–0.0008	–0.0005	–0.0008	–0.0010
4	–0.0016	–0.0008	–0.0007	–0.0009	–0.0005	–0.0005	–0.0004	–0.0005	–0.0004
5	–0.0014	–0.0009	–0.0005	–0.0005	–0.0007	–0.0006	–0.0004	–0.0003	–0.0004
6	–0.0015	–0.0009	–0.0008	–0.0005	–0.0006	–0.0004	–0.0003	–0.0002	–0.0005
7	–0.0014	–0.0009	–0.0005	–0.0004	–0.0004	–0.0003	–0.0002	–0.0003	–0.0003
8	–0.0015	–0.0012	–0.0008	–0.0005	–0.0003	–0.0002	–0.0003	–0.0002	–0.0004
9	–0.0016	–0.0010	–0.0010	–0.0004	–0.0004	–0.0005	–0.0003	–0.0004	–0.0007

Figure 7 Change in k_{eff} for single rod removal in the GBC-32 basket cell for one quadrant of the 17 × 17 fuel assembly with uniform axial burnup of 75 GWd/MTU. The tabulated values are shown beneath the graphical representation.

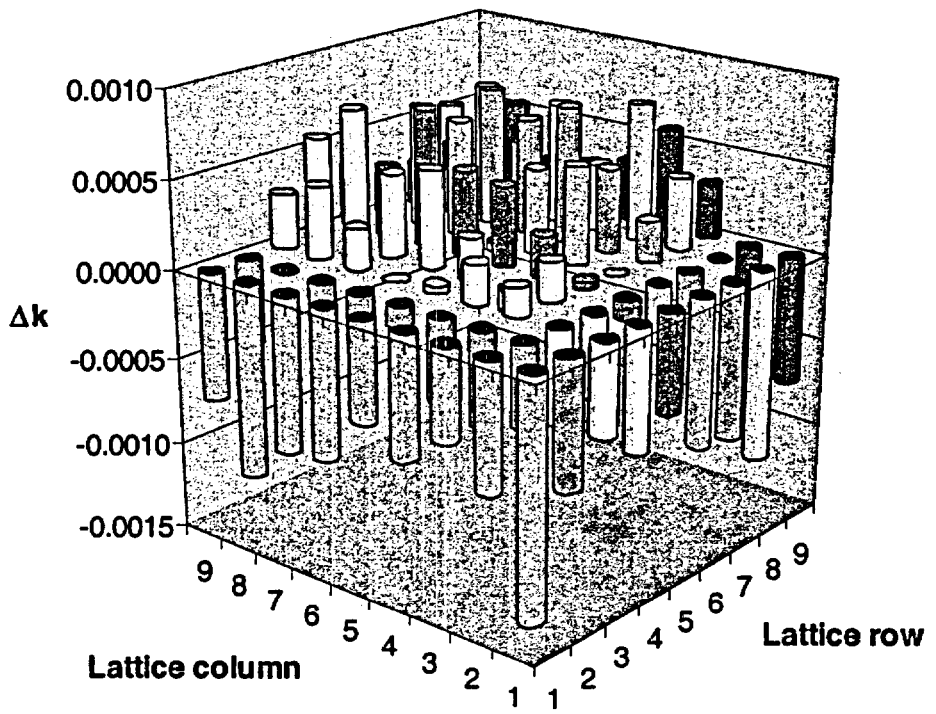

Column/row	1	2	3	4	5	6	7	8	9
1	–0.0014	–0.0007	–0.0005	–0.0007	–0.0006	–0.0009	–0.0009	–0.0011	–0.0007
2	–0.0007	–0.0005	–0.0005	–0.0005	–0.0001	–0.0003	–0.0002	0.0000	–0.0005
3	–0.0005	–0.0005	0.0002	0.0002	0.0000	0.0000	0.0002	0.0004	0.0003
4	–0.0007	–0.0005	0.0002	–0.0001	0.0002	0.0006	0.0005	0.0008	0.0006
5	–0.0006	–0.0001	0.0000	0.0002	0.0005	0.0005	0.0008	0.0004	0.0003
6	–0.0009	–0.0003	0.0000	0.0006	0.0005	0.0000	0.0007	0.0007	0.0003
7	–0.0009	–0.0002	0.0002	0.0005	0.0008	0.0007	0.0008	0.0004	0.0002
8	–0.0011	0.0000	0.0004	0.0008	0.0004	0.0007	0.0004	0.0007	0.0005
9	–0.0007	–0.0005	0.0003	0.0006	0.0003	0.0003	0.0002	0.0005	–0.0001

Figure 8 Change in k_{eff} for single rod removal in the GBC-32 basket cell for one quadrant of the 17 × 17 fuel assembly with axially distributed burnup of 75 GWd/MTU. The tabulated values are shown beneath the graphical representation.

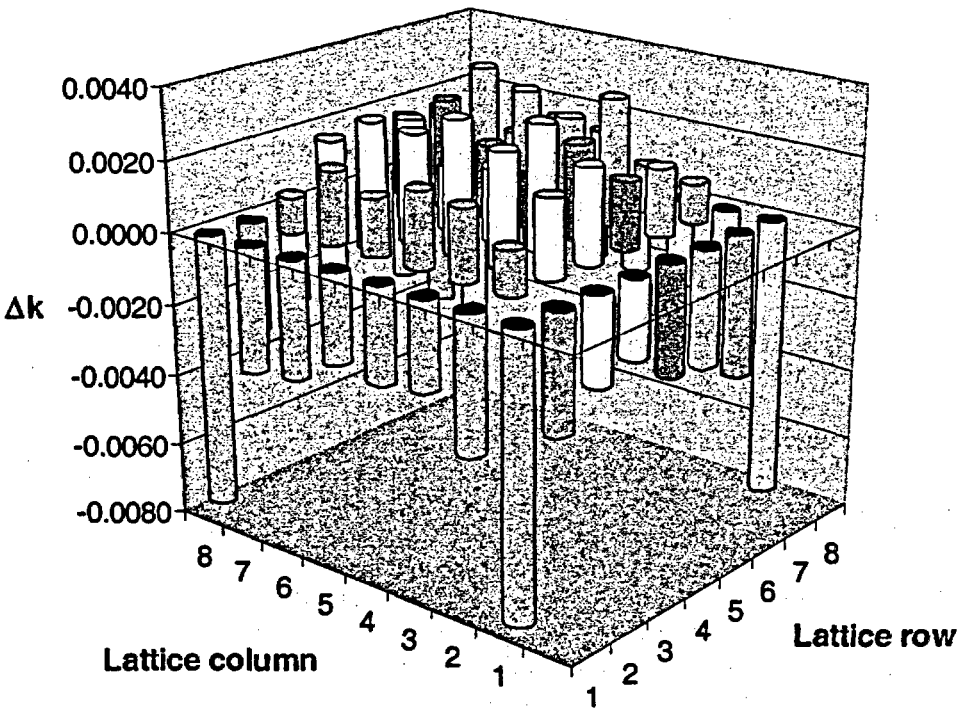

Column/row	1	2	3	4	5	6	7	8
1	–0.0079	–0.0037	–0.0024	–0.0026	–0.0025	–0.0033	–0.0035	–0.0076
2	–0.0033	0.0012	0.0020	0.0021	0.0016	0.0020	0.0010	–0.0030
3	–0.0025	0.0022	0.0031	0.0036	0.0030	0.0030	0.0022	–0.0026
4	–0.0022	0.0026	0.0035	0.0020	0.0017	0.0028	0.0016	–0.0028
5	–0.0031	0.0019	0.0026	0.0014	0.0020	0.0030	0.0022	–0.0019
6	–0.0033	0.0019	0.0035	0.0027	0.0032	0.0036	0.0022	–0.0031
7	–0.0040	0.0011	0.0013	0.0021	0.0022	0.0014	0.0013	–0.0042
8	–0.0079	–0.0025	–0.0025	–0.0024	–0.0023	–0.0025	–0.0034	–0.0078

Figure 9 Change in k_{eff} for single rod removal in the MPC-68 basket cell. The tabulated values are shown beneath the graphical representation.

2.2.1.2 Loss of multiple fuel rods

Due to the extremely large number of possible permutations of the assembly lattice, it is not practical to evaluate all possibilities involving multiple missing rods. Hence, the results from the previous section were used to guide the development of numerous possible cases, in the interest of finding the most reactive situation. For example, removal of rods near an assembly center in a diagonal orientation with guide tubes (or water holes) has the largest positive effect on k_{eff}. For the MPC-24 and GBC-32 basket cells, 80 unique cases were evaluated, with missing rods varying in number and position. For the MPC-68 basket cell, which has significantly fewer possible variations, 40 unique cases were evaluated. In the interest of bounding k_{eff}, each case was calculated with and without the guide tube/water hole material (zirconium) present. The change in k_{eff} (from the reference condition with all rods present) associated with each case in the MPC-24 and MPC-68 casks is shown in Figures 10 and 11, respectively. The maximum increase in k_{eff} is shown to be less than 0.015 with guide/water hole tubes present and less than 0.019 with the guide/water hole tubes removed (replaced with water). For the GBC-32 cask, these calculations were repeated for each of the four fuel conditions described above (i.e., uniform and axially distributed burnup of 45 and 75 GWd/MTU). The results, shown in Figures 12 through 15, demonstrate that in all cases the maximum increase in k_{eff} is approximately 0.015, decreases with burnup, and is increased by the presence of axially distributed burnup, as compared to uniform axial burnup. Some of the cases that resulted in large negative Δk values, which were typically associated with large numbers of missing rods, are not shown in the figures due to the scale. Although all possible permutations were not evaluated, the trend in the results indicates that the existence of significantly more reactive configurations is unlikely. The most reactive configurations involved missing pins (~10% of total) in the inner regions of the assemblies [i.e., central (N–2) × (N–2) positions] oriented in alternating diagonal rows of missing rods with guide tubes/water holes and fuel rods.

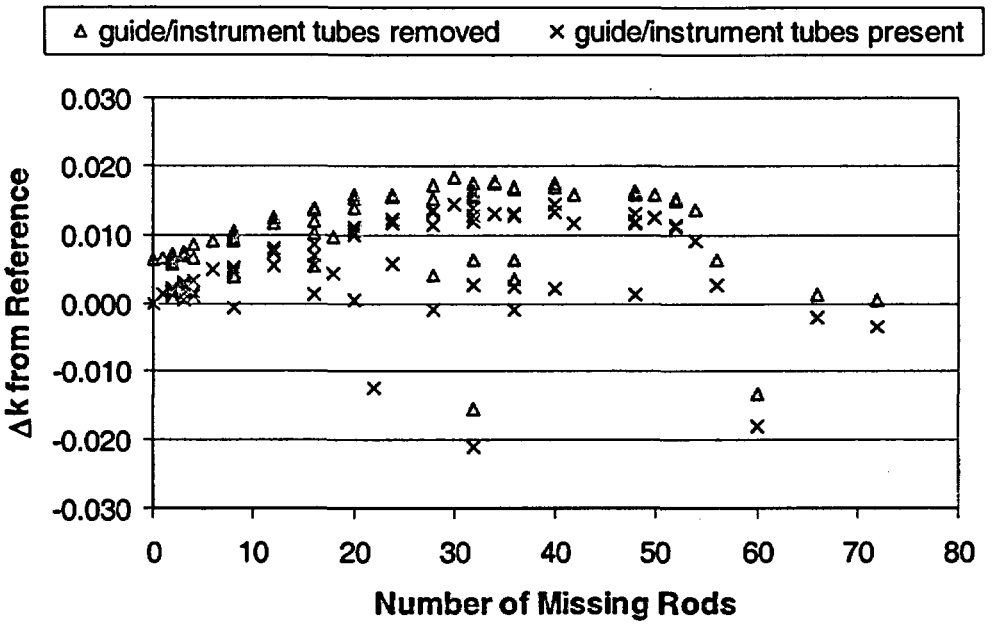

Figure 10 Change in k_{eff} for multiple missing rods in the MPC-24 basket cell

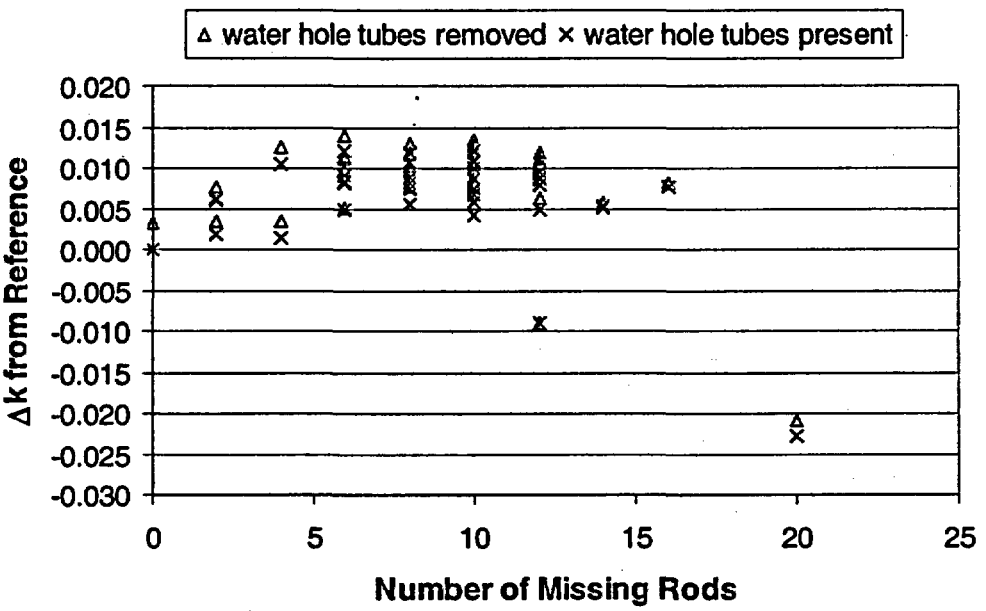

Figure 11 Change in k_{eff} for multiple missing rods in the MPC-68 basket cell

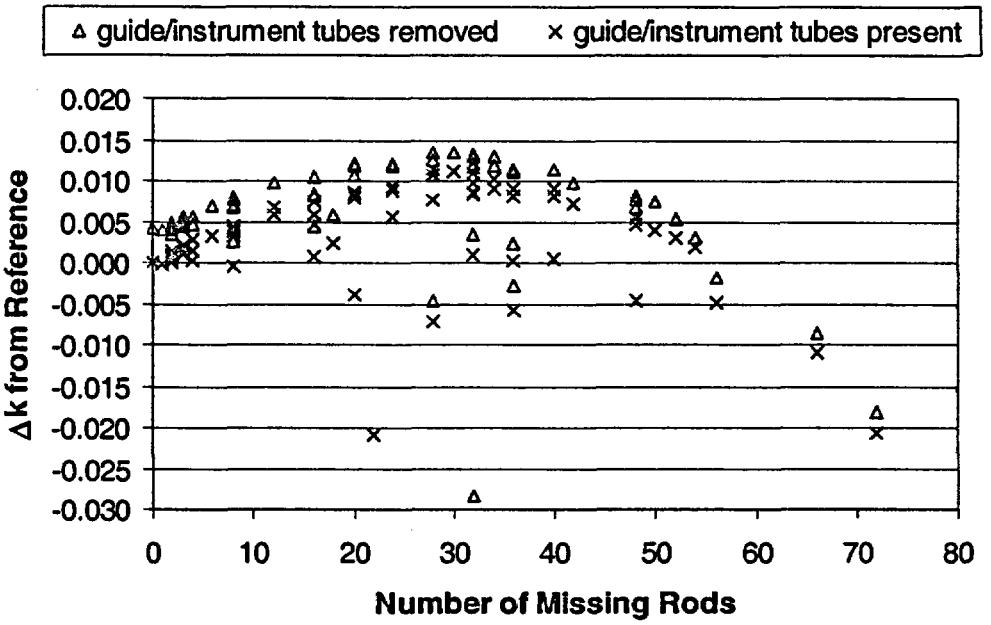

Figure 12 Change in k_{eff} for multiple missing rods in the GBC-32 basket cell with uniform axial burnup of 45 GWd/MTU

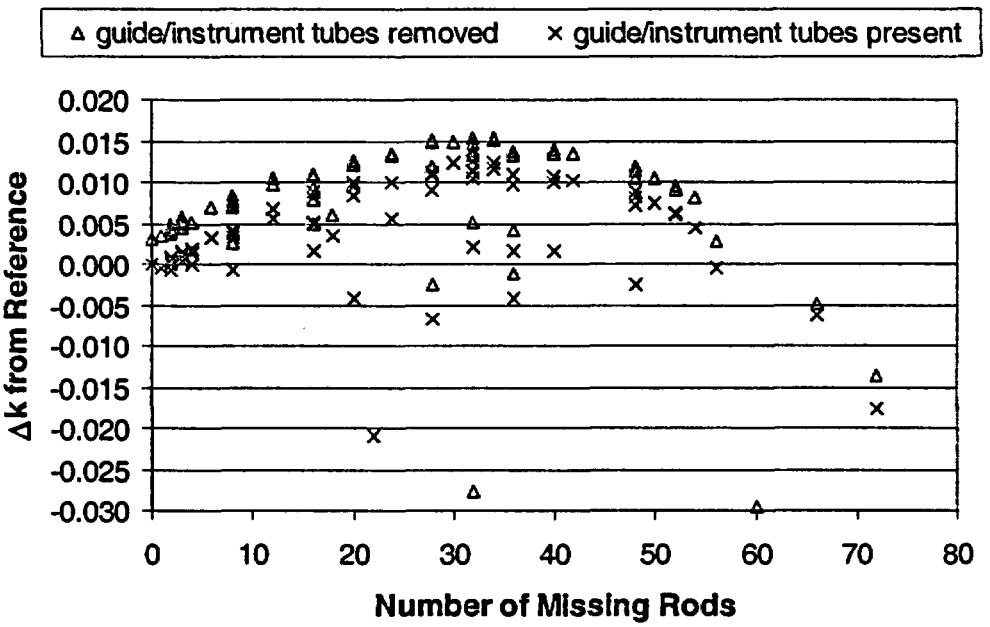

Figure 13 Change in k_{eff} for multiple missing rods in the GBC-32 basket cell with axially distributed burnup of 45 GWd/MTU

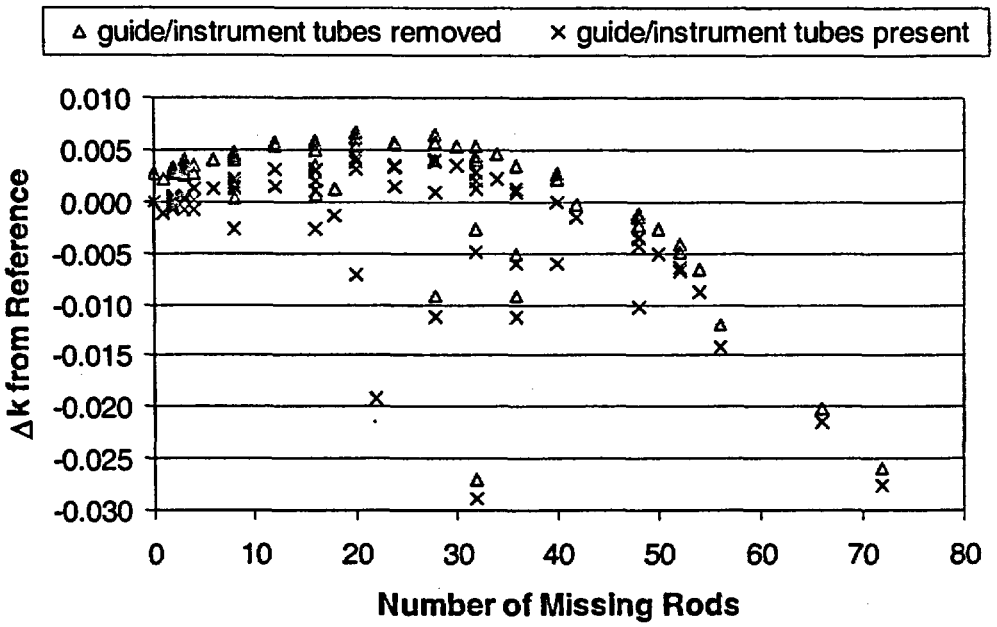

Figure 14 Change in k_{eff} for multiple missing rods in the GBC-32 basket cell with uniform axial burnup of 75 GWd/MTU

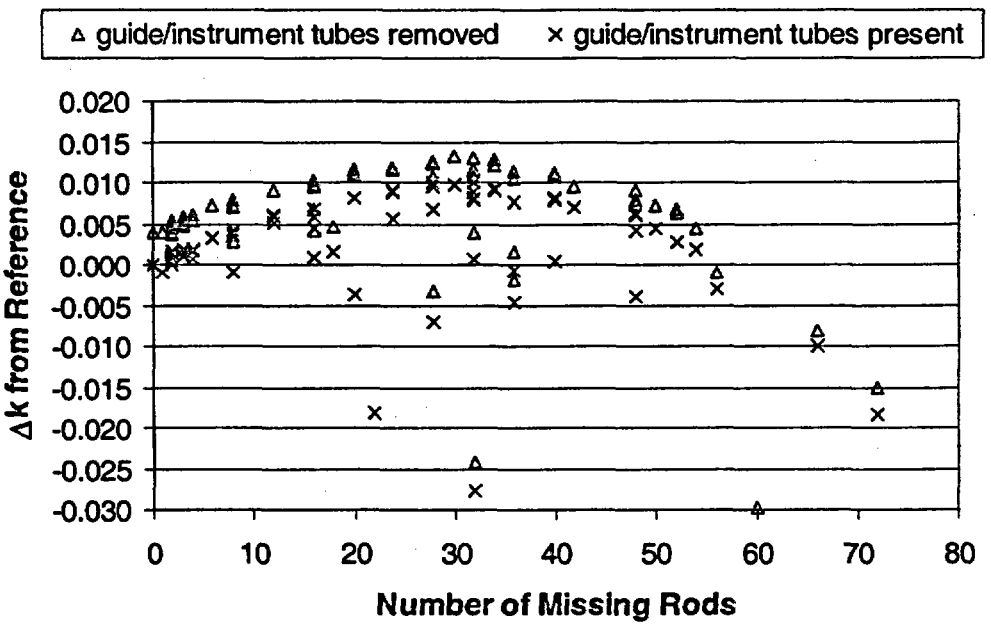

Figure 15 Change in k_{eff} for multiple missing rods in the GBC-32 basket cell with axially distributed burnup of 75 GWd/MTU

2.2.2 Loss of Fuel Rod Cladding

This fuel failure scenario was analyzed by simply taking each full-cask model and removing the fuel cladding from all fuel rods. All other fuel basket and cask hardware, including the BWR assembly channel, remained in the model. The space formerly filled with cladding was filled with water. This provides extra moderation to an otherwise undermoderated system and thus increases the k_{eff} by a substantial amount. The calculated k_{eff} values and increase in k_{eff} relative to each baseline full-cask model are given in Table 4.

Table 4 Results for loss of fuel rod cladding

Cask	k_{eff}	Δk_{eff}
MPC-24	0.9837	+0.0468
GBC-32 (uniform 45)	0.9937	+0.0314
GBC-32 (axial 45)	1.0196	+0.0349
GBC-32 (uniform 75)	0.8511	+0.0258
GBC-32 (axial 75)	0.9213	+0.0344
MPC-68	0.9799	+0.0441

2.2.3 Collapse of Fuel Rods

In this scenario, there was an assumed total collapse of fuel rods and removal of all fuel hardware and cladding, leaving each basket full of fuel pellets at an optimum pitch. The rubble was assumed to be within the volume of the original assembly and thus was in the axial region surrounded by Boral. KENO-VI models of each basket cell were used in order to take advantage of the dodecahedron and dodecahedral array geometry capability of this code. This capability allows the fuel rubble to be easily modeled as a 3-D closely packed array of fuel pellets. The size of the fuel pellets was representative of each type of fuel (PWR and BWR), and the oxide density in the pellets was assumed to remain unchanged. For the PWR fuel casks (MPC-24 and GBC-32), the fuel pellets have an outer diameter of 0.7844 cm and a height of 1.288 cm. The BWR fuel pellets in the MPC-68 cask have an outer diameter of 1.0655 cm and a height of 0.8128 cm. Both types of fuel have an oxide density of 10.522 g/cm^3.

The optimum pitch for a dodecahedral array of fuel pellets was calculated for each basket cell, using the appropriate composition data as given in Table 2. The array of fuel pellets in water was used to fill the original active fuel volume. All cask hardware remained in place, but all assembly hardware, including the BWR assembly channel, was removed. The optimum pitch for fuel pellets in each basket cell, along with the associated fuel volume fraction and change in k_{eff} relative to the baseline basket-cell case, are given in Table 5.

Table 5 Results for collapse of fuel rods

Cask	Optimum pellet pitch (cm)	Fuel volume fraction	Δk_{eff}
MPC-24	1.597	0.216	+0.0563
GBC-32 (uniform burnup of 45 GWd/MTU)	1.587	0.220	+0.0233
GBC-32 (uniform burnup of 75 GWd/MTU)	1.560	0.232	+0.0126
MPC-68	1.678	0.217	+0.1149

2.2.4 Fuel Assembly Slips Above/Below Neutron Poison Panels

This failure scenario involved the loss of the assembly hardware and spacer, allowing the fuel assembly to slip into an axial region with no neutron poison coverage in the basket. As the fuel assembly moves axially, it begins to form an infinite planar region without neutron poison panels. As the thickness of this region increases, the assemblies begin to interact neutronically with each other, and k_{eff} begins to increase. The thickness at which k_{eff} begins to increase varies depending upon many factors, as shown in this section.

To calculate the effect on k_{eff} for this scenario, each basket-cell model was modified to include 30 cm of water below the fuel assembly, followed by steel representing the cask bottom. The steel walls of the basket cell were continuous from the top of the assembly to the cask bottom, but the Boral panels ended at the bottom of the assembly's original axial position. The fuel assembly was then lowered 1 cm at a time until it reached the cask bottom (baseplate). Figure 16 shows the MPC-24 cask with the fuel assembly 20 cm below its original position. For the GBC-32 cask, cases with both uniform and axially-distributed burnup were considered. So that the least burned and therefore most reactive section of the burned assemblies in the GBC-32 cask is dominant in this scenario, the axial burnup profile was inverted. This simulates a transportation accident in which the cask is left upside down and the upper portion of the fuel assemblies slip beyond the Boral panels.

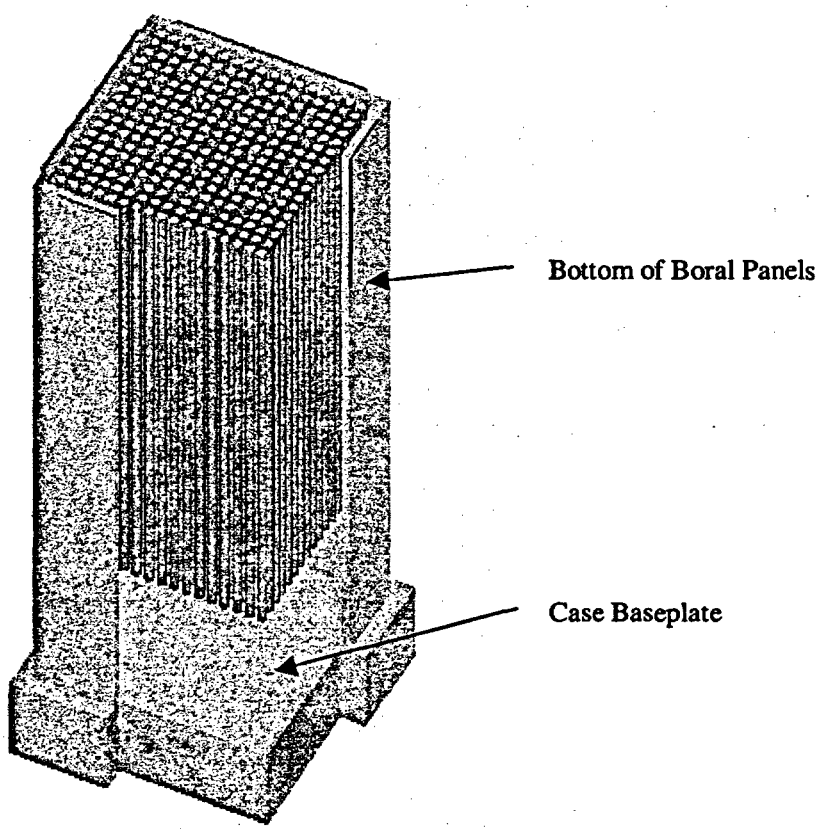

Figure 16 MPC-24 cask showing the fuel assembly below the Boral panels

The maximum value of 30 cm was chosen for this scenario to allow the calculation of clear trends in k_{eff}. However, based on an examination of current cask designs, a maximum value of 20 cm is probably more appropriate for evaluating the worst-case increase in k_{eff} for this scenario. Typical storage/transport casks do not have 30 cm of space between the bottom of the poison panels and the cask baseplate. For the Holtec HI-STAR cask safety analysis report calculations, which were designed for conservatism, the MPC-24 cask model has 10.16 cm of space below the assemblies and the MPC-68 cask model has 18.54 cm. If spacers are to be used, cask-loading procedures would include the insertion of solid spacers above and/or below fuel assemblies, and the failure to include a spacer should be detected during cask loading. It is also unlikely that the spacer could become dislodged in such a way that the assembly could slip below the Boral panels. To determine if the use of 30 cm of water below the assembly would produce results that are significantly different from using 20 cm of water, the MPC-24 cask cases were reevaluated with 20 cm of water followed by the steel baseplate. The values of Δk_{eff} remain consistent with the 30 cm cases up through the 20 cm level. Therefore, it appears that the trend in calculated Δk_{eff} is not affected by the distance to the steel baseplate.

For the MPC-24 cask, no significant increase in k_{eff} occurs until the fuel-pin array is approximately 20 cm below the Boral panels. After that point, k_{eff} rises sharply. For the MPC-68 cask, the calculated k_{eff} stays relatively constant until the fuel-pin array is approximately 13 cm below the Boral panels and then rises to a maximum Δk of +0.0362 at 20 cm below the Boral. For the GBC-32 cask, the trend in calculated k_{eff} depends strongly on whether uniform burnup or axially-distributed burnup is assumed. If uniform burnup is used, the value of Δk_{eff} remains relatively constant until the fuel-pin array is approximately 25 cm below the Boral panels, and then rises slightly to a maximum of +0.01. For the axially-distributed burnup cases, the value of Δk_{eff} begins climbing as soon as the fuel-pin array begins to drop, and reaches a maximum of approximately +0.08. This difference appears because, for the axially-distributed burnup fuel, most of the fission density is present in the top end of the fuel pins. This end was positioned in the basket cell so that it was the first section to emerge from the Boral panels. Graphs showing the calculated k_{eff} as a function of distance below the Boral panels for each of the casks/fuel combinations are given in Figures 17 through 20. The error bars shown represent plus and minus one standard deviation for the Monte Carlo calculation. The results also indicate the large difference in boron loading and basket spacing between the two MPC casks. As described in Section 2.2.3, the MPC-68 cask utilizes higher boron loading than the MPC-24 cask and places the assemblies closer together. When the assemblies in the MPC-68 cask are allowed to slip below the Boral panels, they are much closer together than the assemblies in the MPC-24 cask and better able to interact neutronically. However, the larger impact in the MPC-68 cask may be reduced if the burnable-poison material that would be present in fresh BWR fuel assemblies is included in the model.

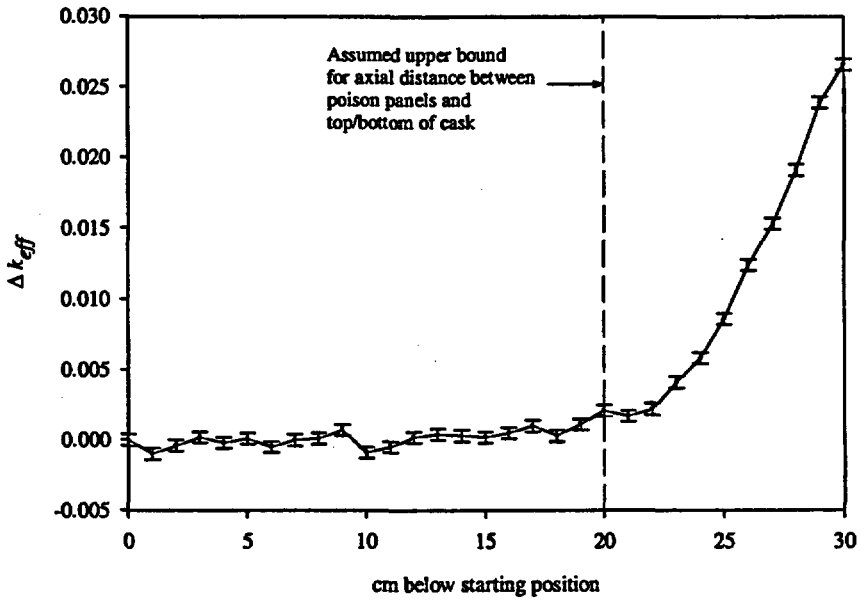

Figure 17 MPC-24 lowering assemblies below neutron poison panels

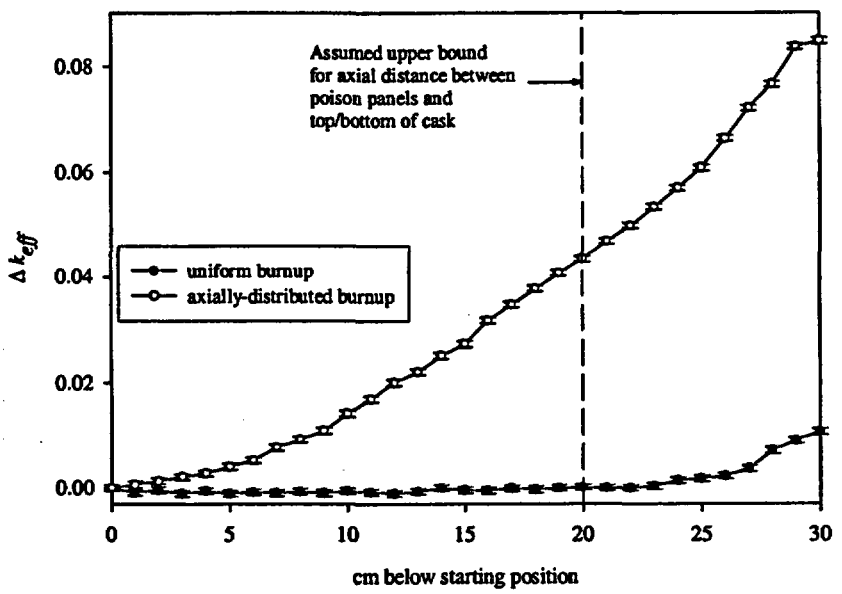

Figure 18 GBC-32 lowering assemblies below neutron poison panels (burnup of 75 GWd/MTU)

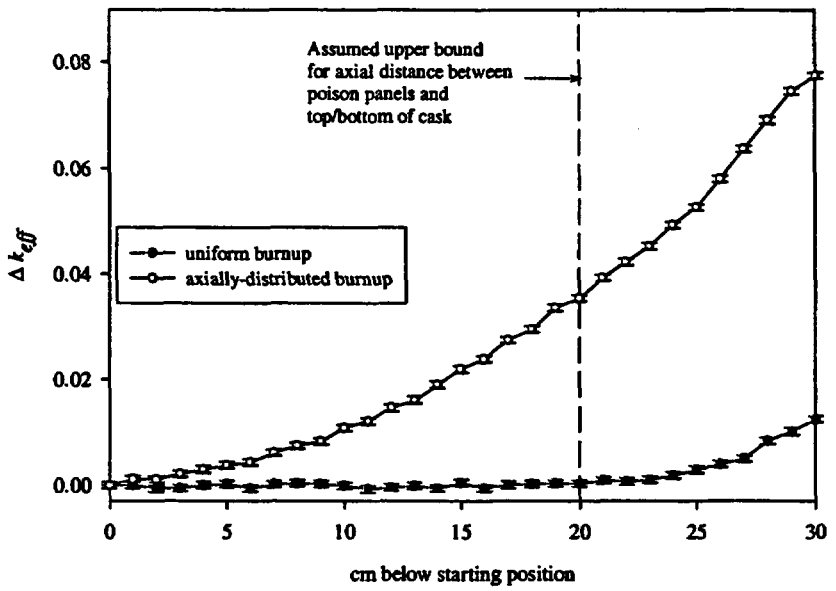

Figure 19 GBC-32 lowering assemblies below neutron poison panels (burnup of 45 GWd/MTU)

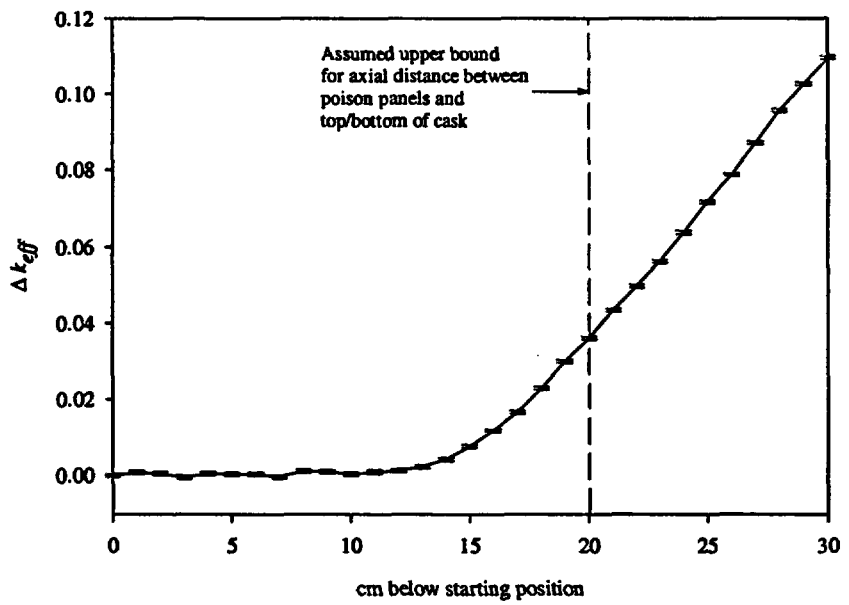

Figure 20 MPC-68 lowering assemblies below neutron poison panels

2.2.5 Determining Optimum Pitch

In this scenario, the fuel rods without cladding were allowed to increase in pitch in a regular lattice within the basket cell until the outer pins reached the basket wall. The pitch was increased further, allowing the outer ring of pins to gradually be removed from the array. The point of maximum k_{eff} was located, which may be compared to the results of scenario 3, where the optimum pitch of the fuel pellets alone is determined. The MPC-24 and MPC-68 basket cells were evaluated for this scenario. For the MPC-68 basket cell, the flow channel was removed along with the fuel rod cladding. Note that the removal of the cladding and flow channel results in an increase in k_{eff} of ~0.04. In both cases, the maximum k_{eff} value for fuel rods without cladding corresponds to the original array expanded such that the outer rods are in contact with the basket-cell walls. Figures 21 and 22 show the trend in k_{eff} as the rod pitch is increased.

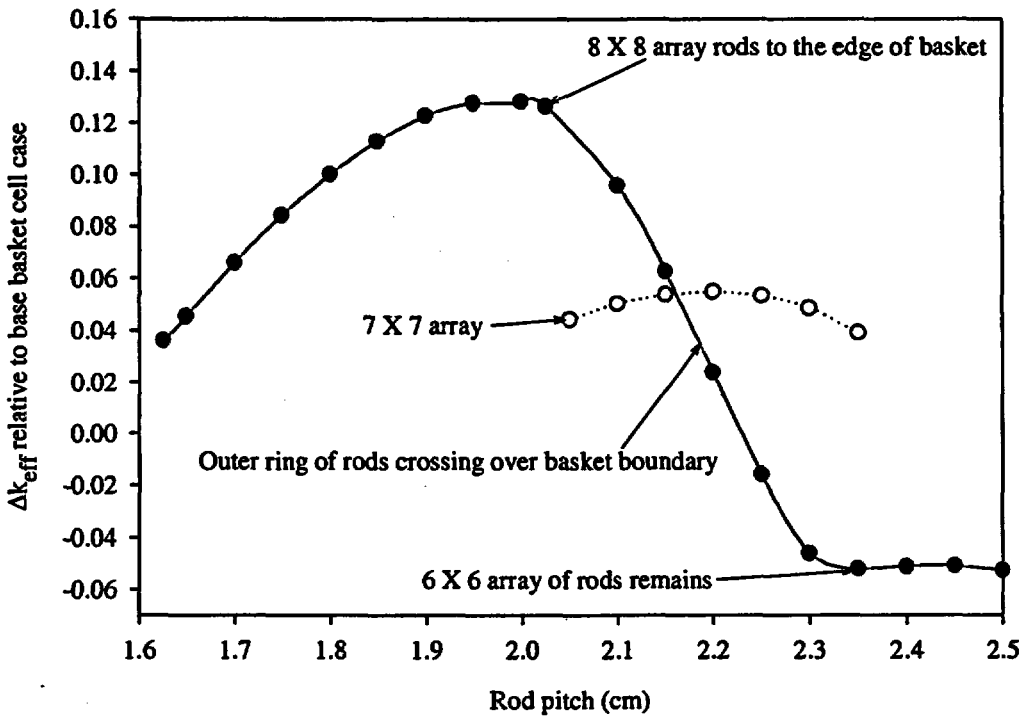

Figure 21 Optimum rod pitch in MPC-68 cask

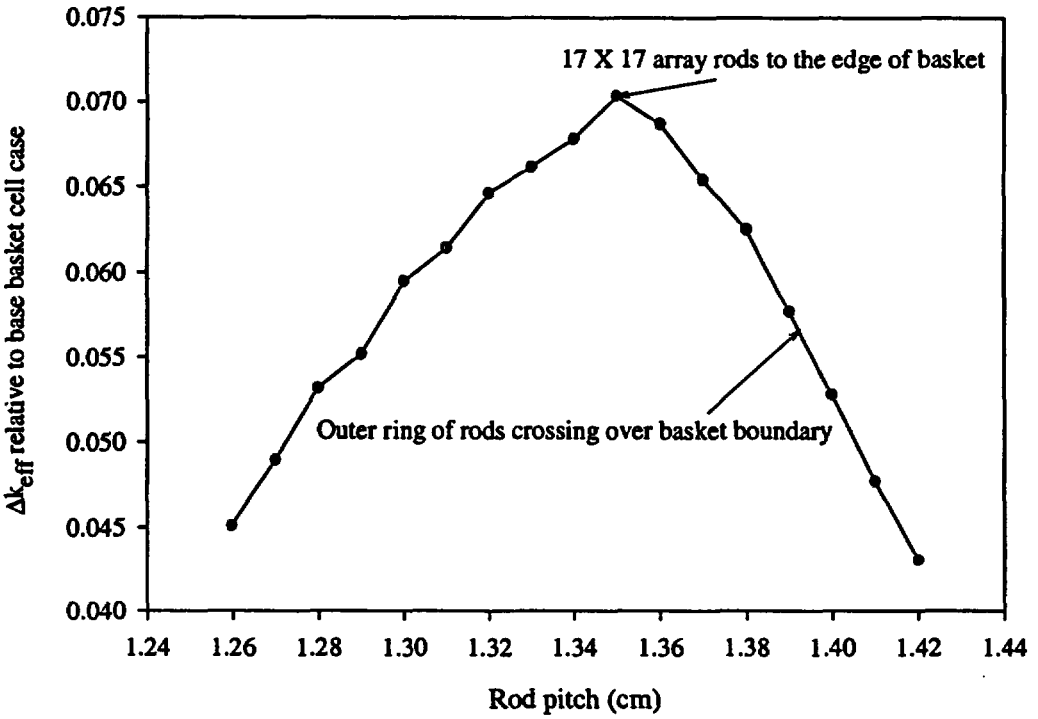

Figure 22 Optimum rod pitch in MPC-24 cask

3 FUEL FAILURE SCENARIOS AFFECTING RADIATION DOSE RATES

Scoping studies are presented in this section to evaluate the effect of potential fuel failure on radiation dose external to an SNF cask. These studies are considered to be scoping in nature because they are based on limited knowledge of failed fuel configurations and include a number of simplifying assumptions (e.g., the analyses assume uniform presence of damaged/failed fuel for each scenario). The impact of each failed fuel scenario on external radiation dose is assessed with respect to the reference (undamaged) configuration.

Potential failed fuel configurations may vary significantly, and hence there is a large degree of uncertainty in defining these configurations. For the shielding analyses in this section, two fuel failure scenarios that would impact external radiation doses are considered. These scenarios are limited to changes in the active fuel configuration and are described below. Although these scenarios may be considered very improbable, the results of their evaluation quantify the effect of severe conditions on external radiation dose and may be useful for bounding the effect of more-likely scenarios.

1. ***Fuel rod collapse resulting in rods being absent from the assembly.*** This scenario evaluates the effect of missing rods by considering both the reduction in the source terms, which would tend to reduce dose rates, and the reduction in fuel region density, which would tend to increase dose rates.

2. ***Collapse of fuel rods.*** This scenario evaluates the effect of gross fuel failure resulting in the collective collapse of all fuel rods and the corresponding compaction of the fuel assemblies.

As the potential for fuel failure increases with burnup, the reference specifications were selected to represent high-burnup PWR fuel in the GBC-32 cask. Consequently, the dose rates for the reference specifications do not meet all of the recommended regulatory limits for dose rates under normal conditions. Rather, focus is given to the difference in the relevant external dose rates with respect to the reference specifications for the scenarios considered. In all cases, the internal and external cask structures are assumed to remain intact, corresponding to normal conditions.

3.1 RADIATION SOURCE SPECIFICATION

The calculation of radiation sources for SNF is typically done for two regions, the active fuel region and the upper and lower hardware regions. These sources consist of neutron and gamma components. The active fuel region includes both components, while the hardware regions contain only gamma source due to the activation of ^{59}Co, an impurity in the steel and Inconel materials used in these regions.

The radiation sources associated with the active fuel region were calculated with the ORIGEN-ARP code,[6] which is functionally equivalent to the SAS2H code,[7] for a Westinghouse 17 × 17 assembly. The cross-section library utilized for the source calculation was the SCALE 44-group library,[8] which is based on ENDF/B-V data with selected nuclides from ENDF/B-VI. Because the fuel failure scenarios considered are focused on damage to the active fuel region, and hence do not impact the fuel assembly hardware, source terms were not calculated for the hardware regions. For the active fuel region, sources were calculated for three enrichment, burnup, and cooling time combinations to enable studies of the dependence of the fuel failure scenarios on variations in source. These combinations include

1. 5 wt % ^{235}U enrichment, 75-GWd/MTU burnup, 5-year cooling;
2. 5 wt % ^{235}U enrichment, 75-GWd/MTU burnup, 20-year cooling; and
3. 4 wt % ^{235}U enrichment, 45-GWd/MTU burnup, 10-year cooling.

3.2 CASK MODEL SPECIFICATION

The cask model used for the shielding studies is a variation of the GBC-32 cask that was used in the previous section for criticality safety studies. Because the GBC-32 cask was originally developed for use in burnup-credit criticality studies, it is not suitable for shielding studies in its original form. To enable relevant shielding studies with the GBC-32 cask, the cask shield body was modified from a single steel component to have the attributes of a realistic storage/transportation cask. The shielding design feature of the modified GBC-32 cask is the cask body, consisting of an inner shell of stainless steel (27 cm thick) surrounded by an outer shell of resin (10 cm thick) for neutron shielding. The stainless steel lid and bottom (35 cm thick) of the cask provide shielding in the axial direction. The impact limiter materials are ignored for conservatism, except that the location of the outer surface of the cask is considered to correspond to the impact limiter boundary. The details of the modified GBC-32 cask design are provided in Ref. 9. Except for the inclusion of the Boral panels in the model used for this study, the model is consistent with that described in Ref. 9. Furthermore, the modeling and analysis approach is consistent with that described in Appendix C of Ref. 9.

The analysis utilized the SCALE 3-D Monte Carlo shielding sequence SAS4,[10] which uses MORSE-SGC[11] for the Monte Carlo simulation. Within this sequence, neutron source multiplication was included. Also, the effect of the axial variation in burnup on the neutron and gamma sources was included by way of the default axial-burnup profiles in SAS4. The shielding calculations utilized the SCALE 27N-18COUPLE library,[8] which is a coupled 27-neutron and 18-gamma group library based on ENDF/B-IV data. The 3-D model is shown in Figure 23 (radial model) and Figure 24 (axial model). The fuel assemblies were homogenized into the basket areas, with the basket structure modeled separately. For the reference case, the model is symmetric about the axial midplane (a requirement of SAS4) and only the bottom of the cask geometry is modeled. Assembly spacers, which are often employed above and below fuel assemblies to approximately center the assemblies within the cask and immobilize the assemblies during transportation, are assumed to be present; however, no credit is taken for the spacer material (i.e., spacer volume is modeled as void).

3.3 ANALYSIS

The shielding analysis was performed by calculating the dose rates at the bottom and radial directions for each scenario and comparing the results to the reference (undamaged) condition. The locations at which the dose rates were calculated correspond to the locations cited in the regulatory guidance for dose rate limits during normal conditions of transport (200 mrem/h at the package surface and 10 mrem/h at 2 m from the accessible surface of the conveyance).

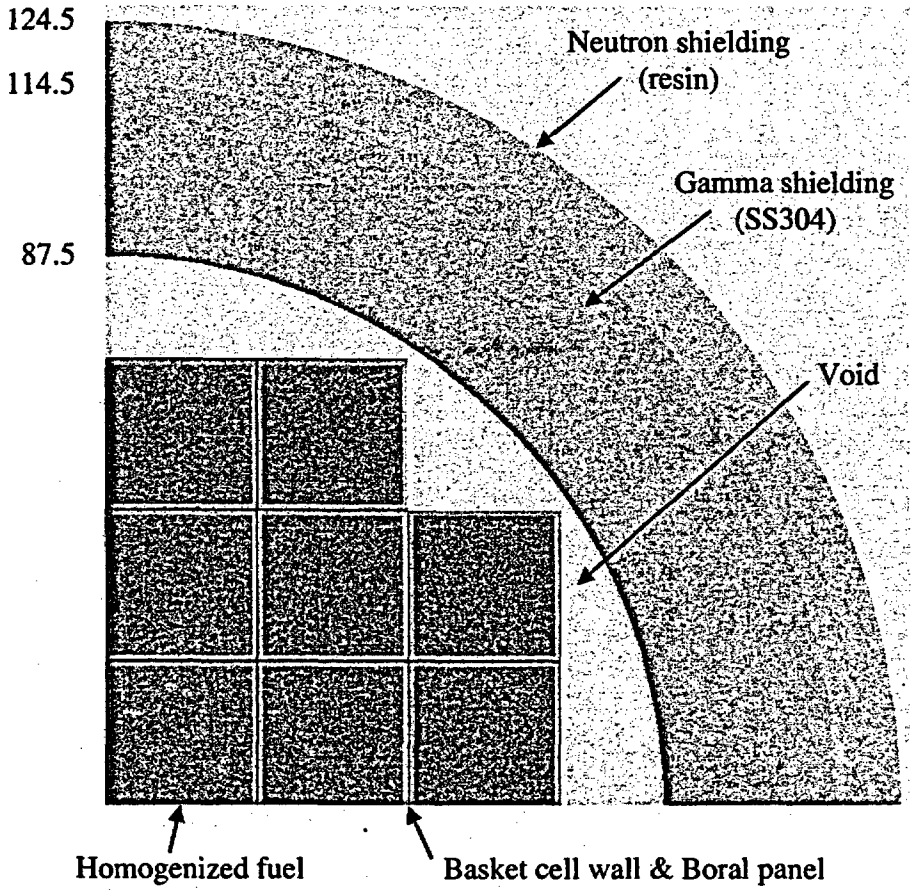

Figure 23 Radial cross section of one-quarter of the SAS4 model of the GBC-32 cask (dimensions in units of centimeters)

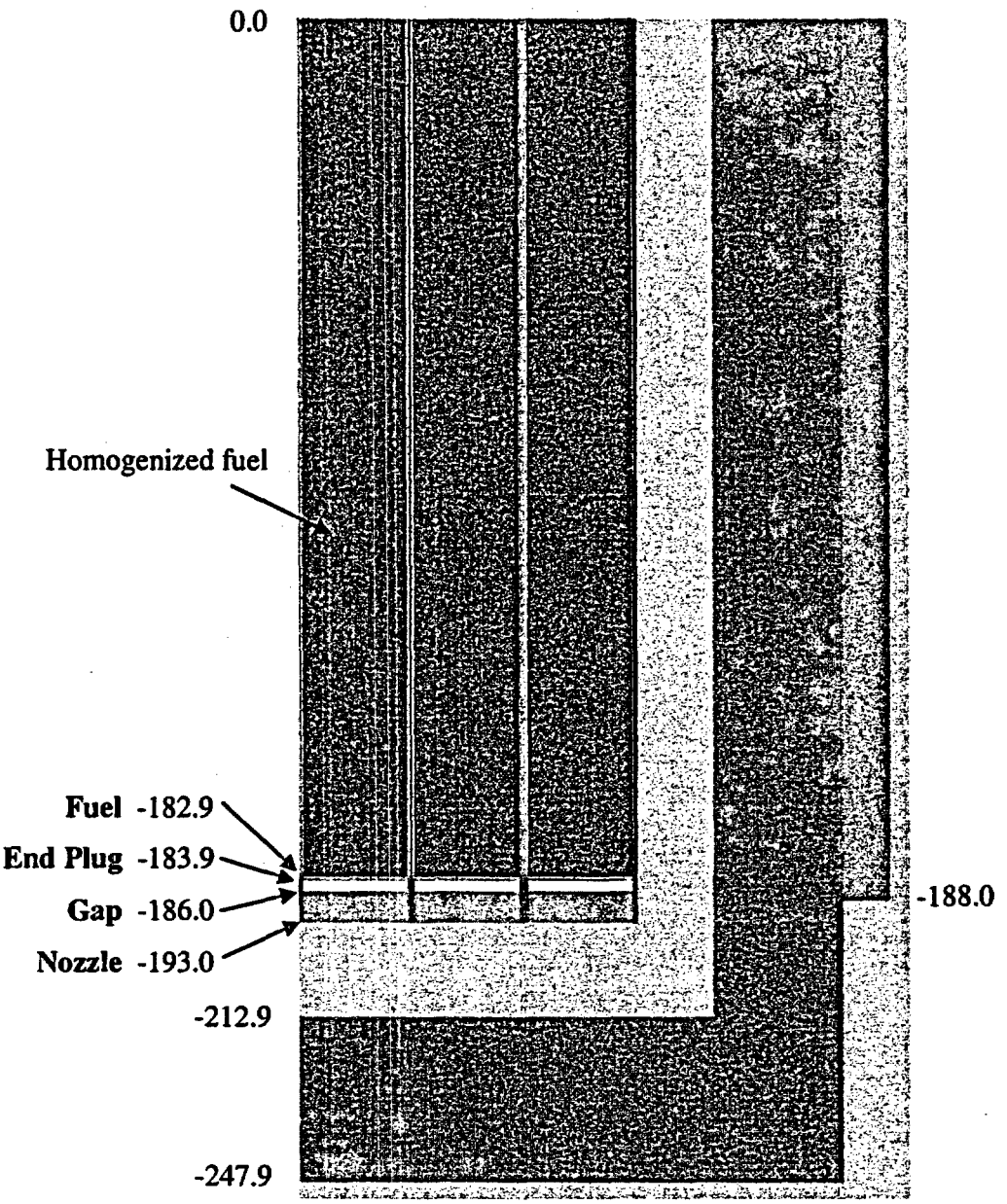

Figure 24 Axial cross section of SAS4 model of the GBC-32 cask (dimensions in units of centimeters)

3.3.1 Reference Conditions

The dose rate profiles along the cask side surface and 2-m locations are shown in Figures 25 and 26, respectively. These dose rates correspond to fuel with 5 wt % ^{235}U initial enrichment, 75-GWd/MTU burnup, and 20-year cooling. Because the failed fuel scenarios to be considered do not involve the fuel hardware and the finding that the hardware regions are of little consequence to total doses for this cask configuration,[9] dose rates due to fuel hardware were not calculated and are not included in the cited values for total dose rate. The location for the side surface doses is the actual outside surface of the neutron shield. The 2-m dose rates correspond to 2 m from the conveyance or a distance of 358 cm from the cask centerline. The dose rates peak at the cask midplane with side surface and 2-m total dose rates of 83 and 18 mrem/h, respectively. In all cases, the statistical uncertainty in the calculated dose rates is <5%.

Both locations have neutron dose rates that are more than a factor of seven higher than the corresponding gamma dose rates. The substantially higher neutron dose is due to the very high burnup considered (i.e., 75 GWd/MTU) and to a lesser extent to the cask design, which is characterized by a greater thickness of gamma shielding material (stainless steel) than neutron shielding material (resin). Previous studies[12,13] have demonstrated that the dominant effect of increasing burnup is the dramatic increase in the spontaneous fission neutron source, primarily from ^{244}Cm. Hence, the neutron dose rate has been shown to increase approximately as burnup to the power of four, while the gamma dose rate increases nearly linearly with burnup. For a combination of enrichment, burnup, and cooling time that is more typical of that which can be accommodated in current transportation casks (e.g., 4 wt % ^{235}U enrichment, 45-GWd/MTU burnup, 10-year cooling), the neutron dose rates are less than a factor of 2 greater than the gamma dose rates.

The dose rate profiles along the bottom surface and 2-m locations are shown in Figures 27 and 28, respectively. These dose rates correspond to 5 wt % ^{235}U enrichment, 75-GWd/MTU burnup, and 20-year cooling. For these calculations, the material in the impact limiter is ignored (i.e., assumed void). However, the surface doses correspond to the boundary of the impact limiter and the 2-m dose rates correspond to a location 2 m from the impact limiter surface. The dose rates peak at the center of the cask with bottom surface and 2-m total dose rates of 145 and 27 mrem/h, respectively. Along the cask bottom, the total dose rate is dominated by the neutron dose rate because there is no neutron shielding material present along the cask bottom. This disparity between neutron and gamma dose rates is increased further because, as discussed above, the neutron source/dose increases much more dramatically with fuel burnup than the gamma source/dose does.

3.3.2 Fuel Rod Collapse/Missing Fuel Rods

This scenario investigates the effect of missing rods by considering both the reduction in the radiation source terms, which tends to reduce dose rates, and the reduction in fuel region density, which tends to increase dose rates. To model this scenario, various numbers of rods were simply assumed to be absent from the assembly lattice. The specific cases considered included 5, 10, and 20% of the fuel rods absent, which corresponds to missing 13, 26, and 53 rods, respectively. The homogenized fuel region compositions and source terms were calculated and used for each of these three cases.

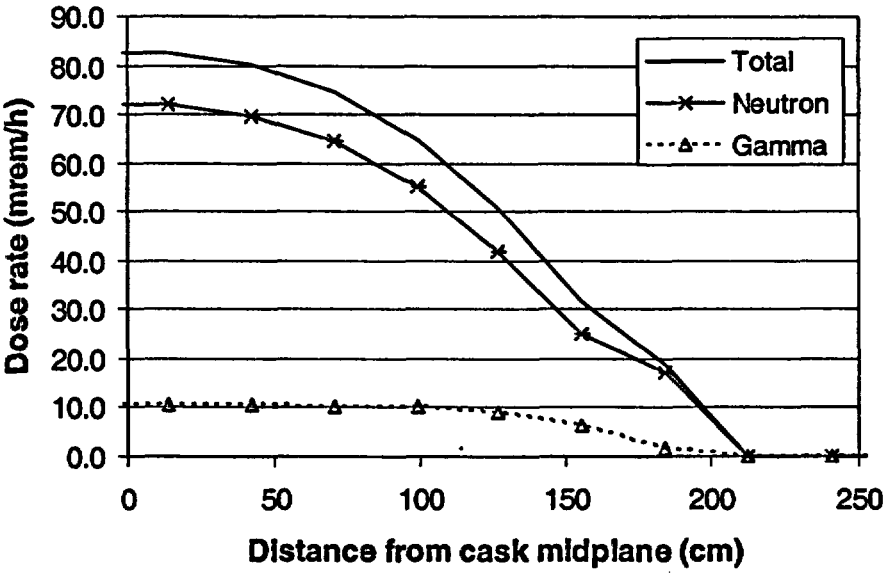

Figure 25 Surface dose rate profiles along the side of the GBC-32 cask (5 wt % ^{235}U enrichment, 75-GWd/MTU burnup, 20-year cooling)

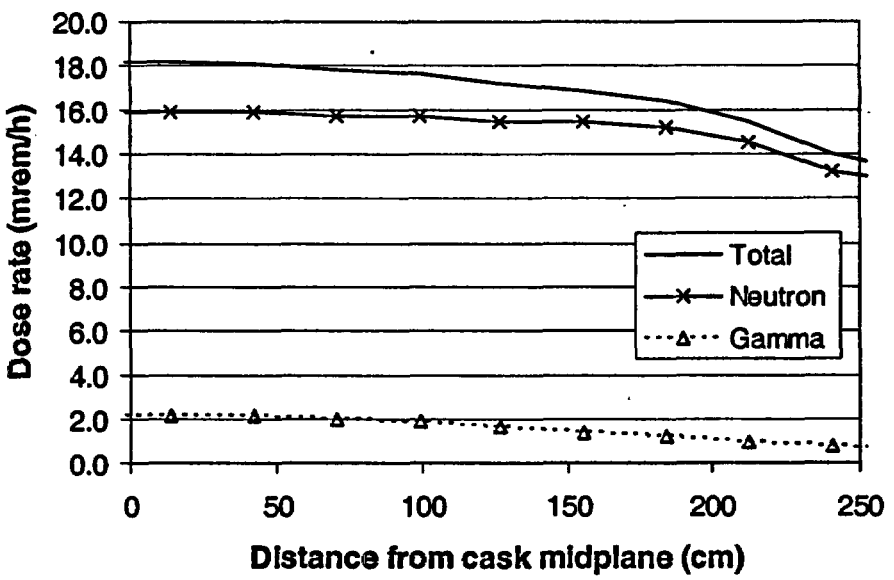

Figure 26 Dose rate profiles at 2 m from the side conveyance surface of the GBC-32 cask (5 wt % ^{235}U enrichment, 75-GWd/MTU burnup, 20-year cooling)

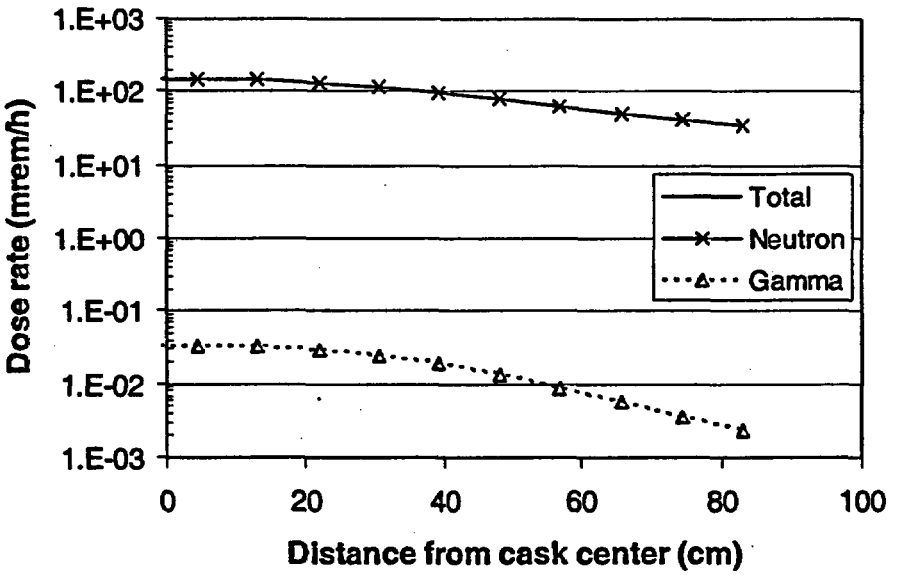

Figure 27 Surface dose rate profiles along the bottom of the GBC-32 cask (5 wt % ^{235}U enrichment, 75-GWd/MTU burnup, 20-year cooling). Note that the neutron and total dose rate curves are indistinguishable.

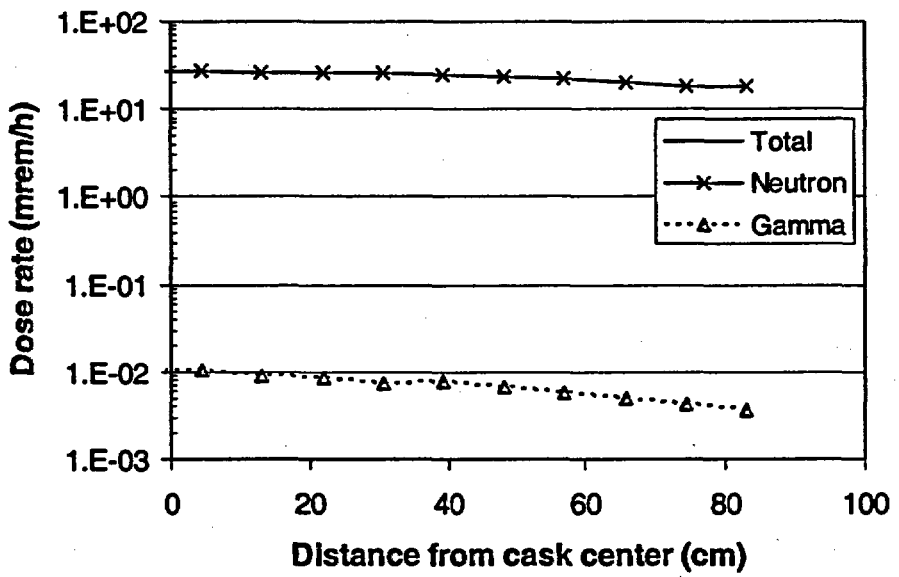

Figure 28 Dose rate profiles at 2 m from the bottom of the GBC-32 cask (5 wt % ^{235}U enrichment, 75-GWd/MTU burnup, 20-year cooling). Note that the neutron and total dose rate curves are indistinguishable.

The absence of fuel rods reduces external dose rates. A comparison of the dose rate profiles along the cask side surface for the reference condition and the case with 5% of the rods missing is shown in Figure 29. These dose rates correspond to fuel with 5 wt % ^{235}U initial enrichment, 75-GWd/MTU burnup, and 20-year cooling. Because this failed fuel scenario does not involve the fuel hardware, the dose rates due to fuel hardware would remain the same. Therefore, these values were not calculated and are not included in the cited values for total dose rate. The total and neutron dose rate profiles along the bottom surface are shown in Figure 30. The gamma dose rates at the bottom are several orders of magnitude lower than the neutron dose rates and hence are not shown.

To more clearly show the impact of missing rods, the total dose rate profiles along the cask side surface and bottom surface are shown in Figures 31 and 32, respectively. For all cases and dose rate locations considered, the absence of fuel rods results in a reduction in the external dose rates; the dose rates decrease with increasing numbers of missing rods. The effect of missing rods was also evaluated for the different combinations of initial enrichment, burnup, and cooling time listed in Section 3.1, and the above conclusions were not found to be dependent on variations in these combinations. Although calculations were not performed with other cask designs, it is anticipated that the above conclusions are not sensitive to the cask design.

3.3.3 Collapse of Fuel Rods (Fuel Rubble)

This scenario evaluates the effect of gross fuel failure resulting in the collective collapse of all fuel rods and the corresponding compaction of the fuel assemblies. This scenario is notably more complicated than the missing rods scenario, and hence the evaluation of this scenario requires a number of important assumptions to be made. Questions such as the following must be considered: (1) How dense is the fuel rubble (i.e., how densely does the fuel compact)? (2) Is the axial-burnup variation maintained in the fuel rubble? (3) Where is the fuel rubble located? Considering the large uncertainty in the fuel failure/damage mechanisms, there are no clear answers to these questions. Hence, relatively simple, rational assumptions are employed here for these conditions to enable a basic evaluation of this scenario. Because the fuel rods are initially positioned vertically, are constrained laterally by the basket-cell walls, and are assumed not to shatter into very small pieces, it is assumed here that the fuel rubble is not in a tightly compacted mass. Instead, the fuel rubble is assumed to be 50% void by volume, which corresponds to a reduction in fuel height of ~25%. Considering that the potential fuel collapse could be associated with a variety of transportation accident conditions, the axial-burnup variation in the rubble is assumed to be uniform. Finally, consistent with a basic assumption in this report, the fuel rubble is assumed to be contained within the original active fuel volume, albeit in the lower portion of the original volume. Although one could imagine situations in which small portions of the fuel rubble fall down into the regions that are primarily occupied by the fuel hardware and fuel assembly spacers (where used), proper representation of such configurations requires an advanced knowledge of the potential fuel failure configuration and hence is not considered here. Finally, note that the fuel rubble is assumed to settle in the bottom axial portion of the original active fuel volume; conditions for fuel rubble settling in a horizontal position are not anticipated to have a significant impact on dose rates and are not evaluated here.

Regarding the calculational models for this scenario as compared to the reference conditions, the homogenized fuel composition for the fuel rubble was calculated and utilized, the active height of the fuel region was reduced, the axial variation in burnup was changed to uniform, and the total source terms remained unaffected. While the reference configuration model is symmetric about the midplane (a requirement of SAS4), the reduction in fuel region height results in axial asymmetry about the cask midplane. Therefore, to evaluate this scenario with SAS4, axial symmetry was modeled/assumed about the fuel rubble midplane. Based on the height of the fuel rubble region, this assumption was judged to be valid for this evaluation; however, the validity of this assumption degrades as the height of the fuel region

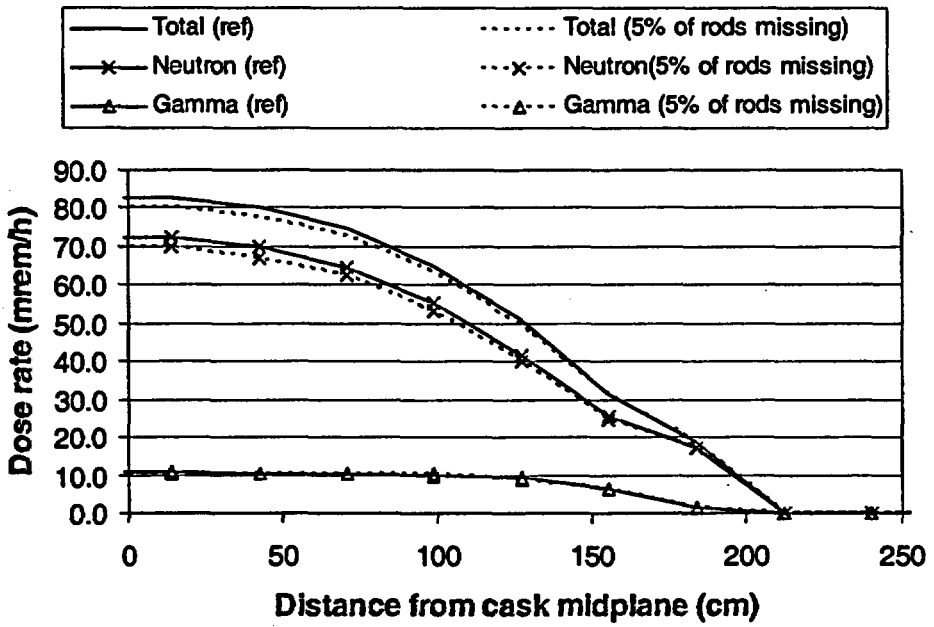

Figure 29 Effect of missing 5% of the fuel rods on surface dose rate profiles along the side of the GBC-32 cask (5 wt % ^{235}U enrichment, 75-GWd/MTU burnup, 20-year cooling)

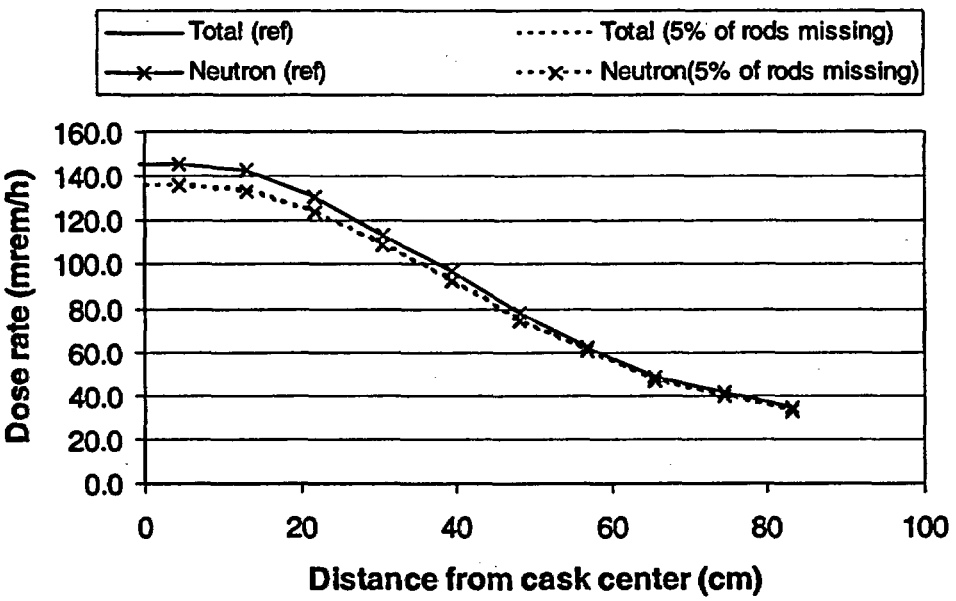

Figure 30 Effect of missing 5% of the fuel rods on dose rate profiles along the bottom surface of the GBC-32 cask (5 wt % ^{235}U enrichment, 75-GWd/MTU burnup, 20-year cooling). Note that the dose rate curves for the two cases are virtually indistinguishable.

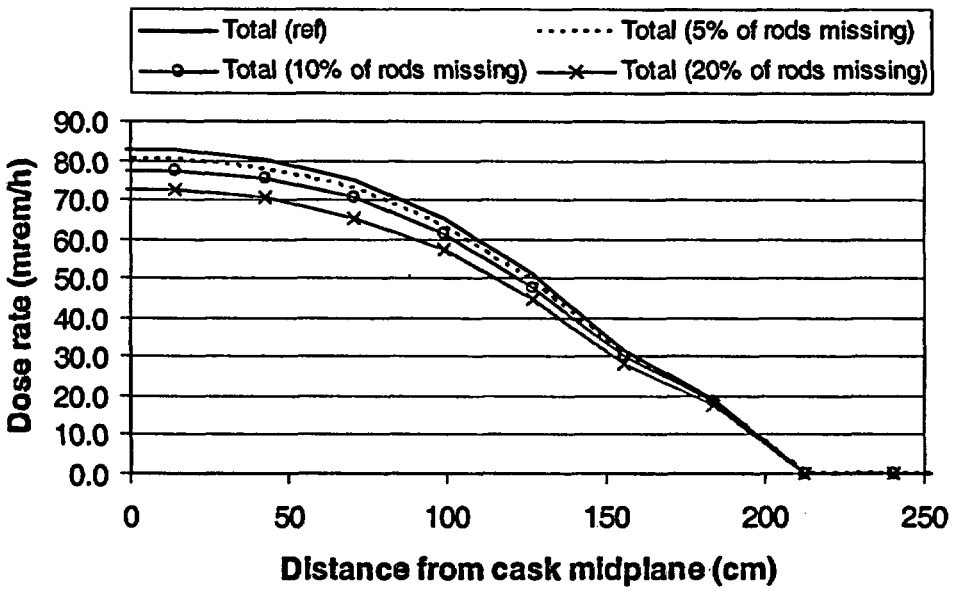

Figure 31 Effect of missing fuel rods on total surface dose rate profiles along the side of the GBC-32 cask (5 wt % ^{235}U enrichment, 75-GWd/MTU burnup, 20-year cooling)

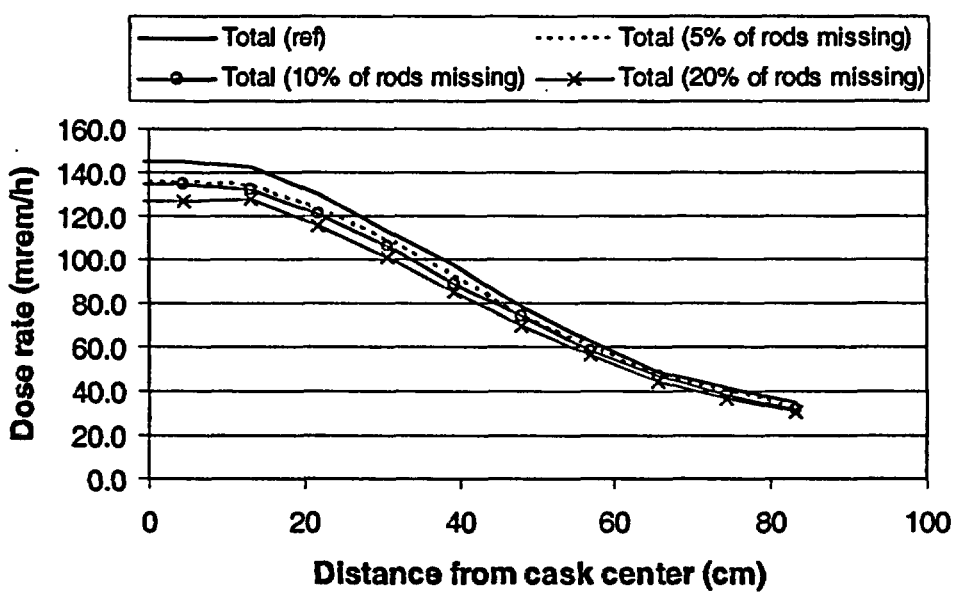

Figure 32 Effect of missing fuel rods on dose rate profiles along the bottom surface of the GBC-32 cask (5 wt % ^{235}U enrichment, 75-GWd/MTU burnup, 20-year cooling)

decreases. Evaluation of scenarios involving significantly greater compaction requires the use of something other than SAS4 for the analysis. After the axial symmetry location was moved, it became necessary to perform separate radial calculations for the top and bottom halves of the fuel rubble to calculate the complete radial dose rate profiles over the bottom half of the cask.

The effect of fuel collapse on dose rate profiles along the cask side surface is shown in Figure 33. These dose rates correspond to fuel with 5 wt % ^{235}U initial enrichment, 75-GWd/MTU burnup, and 20-year cooling. The dose rate profiles along the bottom surface are shown in Figure 34. The most important characteristics of this scenario are the increase in fuel region density and the uniform axial-burnup/source distribution. The impact of the latter characteristic, which effectively moves more source from the axial center region into the lower regions (particularly neutron source; recall that neutron source increases approximately as burnup to the power of four), is evident in both figures. While the peak side surface dose rate is lower for the collapsed fuel than the reference condition, total dose rates in the lower side regions are increased. Neutron peak dose rates at the 2-m location were found to increase by nearly a factor of two. The total/neutron surface and 2-m dose rates along the cask bottom were found to increase by a factor of approximately five as compared to the reference case.

The effects of this scenario are dominated by the assumption that the fuel burnup/source is axially uniform, effectively resulting in the movement of greater neutron source from the center to the end regions of the fuel. This point is shown in Figures 35 and 36, which compare side and bottom surface dose rates, respectively, for this scenario to those of the reference fuel configuration with uniform axial burnup assumed. While the dose rates for this collapsed fuel scenario are slightly higher than the reference dose rates due to the increase in source density, the dose rates are very similar in shape and magnitude.

Because the effects of this scenario are dominated by the movement of greater neutron source to the lower region of the fuel, the effects are notably less for lower burnups and will be somewhat cask dependent (e.g., casks with greater axial neutron shielding will be less sensitive to this condition). Finally, note that the dose rates due to fuel hardware were not calculated and are not included in the cited values for total dose rate. However, the fuel hardware would be dislocated in this scenario. Thus, while the source from the fuel hardware would not change, the dose rate from the fuel hardware would be affected by the change in position.

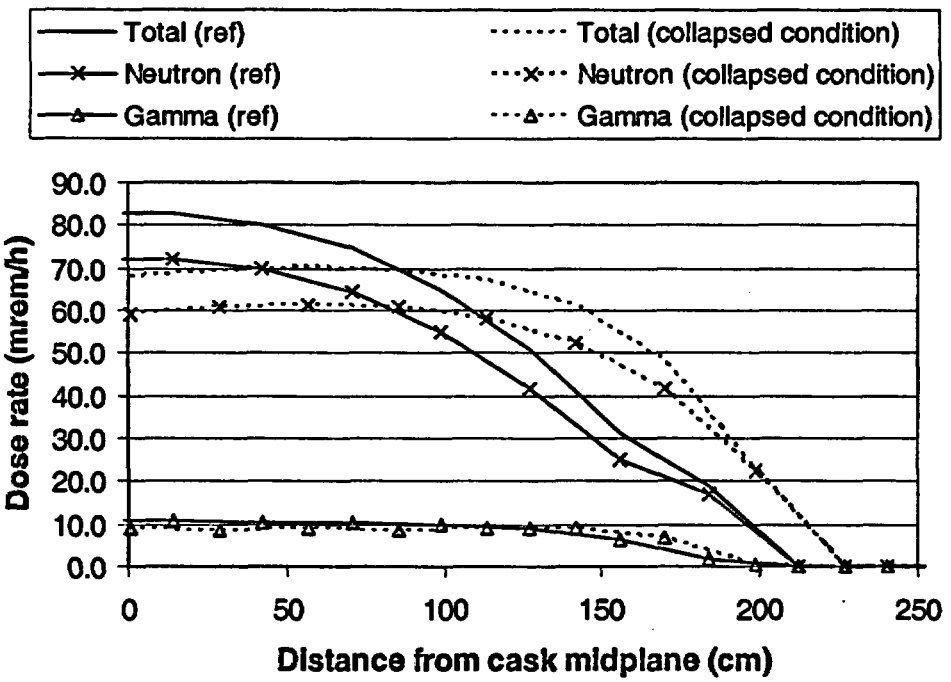

Figure 33 Effect of fuel collapse on surface dose rate profiles along the side of the GBC-32 cask (5 wt % ^{235}U enrichment, 75-GWd/MTU burnup, 20-year cooling)

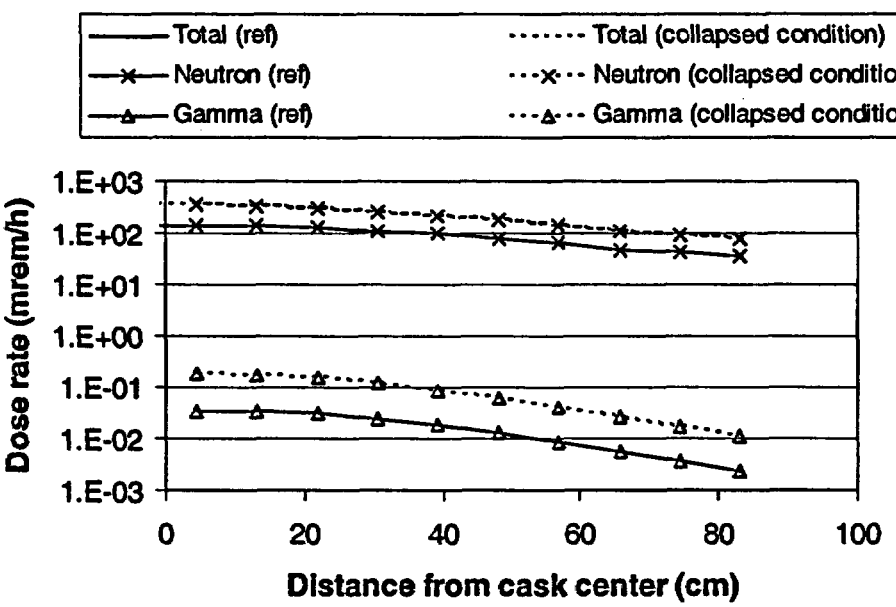

Figure 34 Effect of fuel collapse on surface dose rate profiles along the bottom of the GBC-32 cask (5 wt % ^{235}U enrichment, 75-GWd/MTU burnup, 20-year cooling). Note that the neutron and total dose rate curves are indistinguishable.

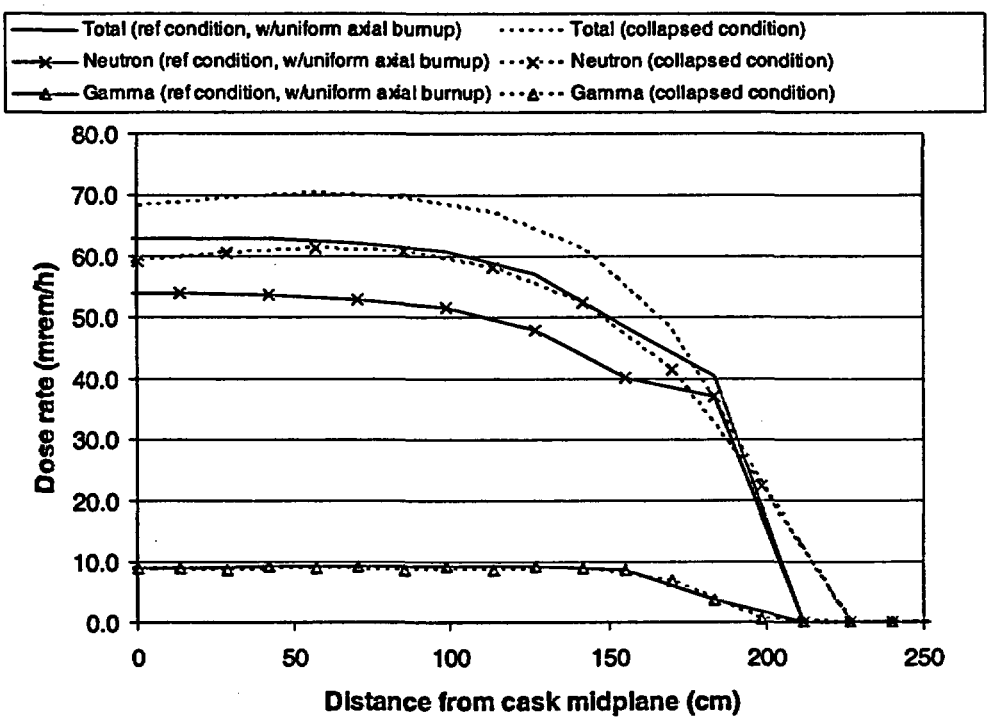

Figure 35 Comparison of surface dose rate profiles along the side of the GBC-32 cask (5 wt % ^{235}U enrichment, 75-GWd/MTU burnup, 20-year cooling)

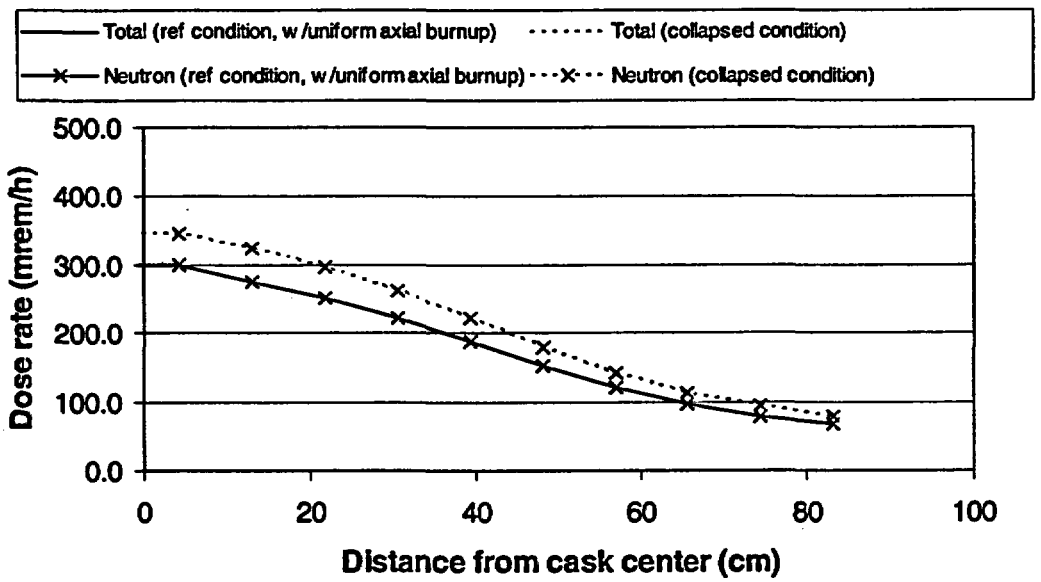

Figure 36 Comparison of surface dose rate profiles along the bottom of the GBC-32 cask (5 wt % ^{235}U enrichment, 75-GWd/MTU burnup, 20-year cooling)

4 CONCLUSIONS

Irradiation of fuel and clad to high-burnup increases the potential for failure during normal and accident scenarios involving transport and storage casks. This report presents scoping studies to investigate and quantify the consequences of potential fuel failure on criticality safety and external radiation dose rates for SNF transport and storage casks.

Five different fuel failure scenarios were evaluated for their effect on criticality safety. Many of the assumptions used in the calculational models were chosen for their maximum effect on the reactivity of the system. These assumptions include full water flooding of the casks, no fuel assembly hardware, and uniform failure of fuel in the cask. The assumed failed fuel configurations represent a theoretical limit beyond credible conditions.

The maximum increase in k_{eff} associated with each of these scenarios for each cask is listed in Table 6.

Table 6 Maximum increase in k_{eff} for each fuel failure scenario

Fuel failure scenario	MPC-24 cask model (fresh fuel)	GBC-32 cask model (45-GWd/MTU axial burnup)	MPC-68 cask model (fresh fuel)
1. Single missing rod	0.0013	< 0.0010	0.0036
Multiple missing rods	0.0140	0.0130	0.0120
2. Cladding removed from all rods	0.0468	0.0349	0.0441
3. Fuel rubble (no cladding material present)	0.0563	0.0233*	0.1149
4. Assembly slips 20 cm above or below neutron poison panels	0.0021	0.0435**	0.0362
5. Variation in pitch (without cladding)	0.0703	N/C	0.1225

N/C = not calculated.
*Uniform axial burnup.
**75 GWd/MTU axially-distributed burnup.

In scenario 1, the removal of a single fuel rod causes an increase in k_{eff} of less than 0.4%. The simultaneous removal of multiple rods resulted in a maximum increase in k_{eff} of slightly less than 1.5%. The removal of all fuel rod cladding results in an increase in k_{eff} of 3.5–5%. Fuel failure scenario 3 (fuel rubble) has a large effect on criticality safety, with an increase in k_{eff} of greater than 10% in the MPC-68 cask model. This increase is significantly larger than that seen with the MPC-24 cask model for the same scenario. The scenario that has the largest effect on criticality safety is scenario 5, which involves variation in rod pitch without cladding present.

In the base basket-cell models, the energy of average lethargy causing fission is 0.2159 eV for the MPC-24 model and 0.2945 eV for the MPC-68 model. The BWR fuel assemblies in the MPC-68 model are

less moderated than the PWR assemblies in the MPC-24 model and are therefore more sensitive to increases in thermalization of the neutrons. Also, the MPC-68 cask utilizes higher boron loading than the MPC-24 cask and does not include a water gap to act as a flux trap between assemblies. When the assemblies in the MPC-68 cask are allowed to slip below the Boral panels, they are much closer together than the assemblies in the MPC-24 cask and better able to interact neutronically. The large impact of the Boral panels in scenario 4 may be reduced if the burnable poison material that would be present in fresh BWR fuel assemblies is included in the model. In the future, studies of similar scenarios with varying amounts of burnable poison in fresh BWR fuel assemblies and with burned BWR fuel assemblies could yield results that are appropriate for evaluating consequences of BWR fuel failure in an actual cask design.

For the evaluation of external dose rates, scenarios involving missing fuel rods and fuel rubble were considered. For all burnup, enrichment, and cooling time combinations considered, the absence of some fuel rods resulted in a decrease in external dose rates at all relevant locations. In contrast, the scenario involving fuel rubble led to notable increases in total dose rate at the side 2-m location and the bottom surface and 2-m locations. The effects of this scenario are dominated by the assumption that the failed fuel burnup/source is uniform, effectively resulting in the movement of greater neutron source from the central to the end regions of the fuel.

Current casks have limits on the number and placement of known damaged or failed fuel assemblies in the cask to control the potential severity of accident events. In addition, the extent and uniformity of the fuel damage assumed in this study represents a theoretical limit. Therefore, evaluation of a specific design will require the establishment of the appropriate configuration for that design.

5 RECOMMENDATIONS FOR FUTURE WORK

The studies presented in this report may be characterized as scoping in nature because they are based on limited knowledge of failed fuel conditions and configurations and include a number of assumptions that are beyond credible (e.g., the analyses assume uniform presence of damaged/failed fuel for each failure scenario). However, these studies quantify the impact of many relevant failure configurations and identify those scenarios that most negatively impact safety, thereby providing a basis for decision making with regard to failure potential and a foundation to direct future efforts in this area. Based on the findings of this work and the inability of materials experts to definitively characterize potential fuel failure conditions, additional work is recommended to more completely and accurately address the safety concerns related to the consequences of potential fuel failure. Building on the results of this present work, future work should further evaluate the most plausible scenarios by incrementally moving towards credible conditions. Specific recommendations for future work include the following:

1. For all plausible scenarios, incrementally evaluate the effect from partial loading of failed fuel. For criticality safety, evaluate the effect of including an increasing number of failed assemblies loaded from the cask center outward. For external dose rates, evaluate the effect of including an increasing number of failed assemblies loaded from the cask periphery inward.

2. For evaluation of criticality safety with loss of fuel rod cladding, progressively remove cladding from fuel rods, beginning in the assembly center and moving outward based on rows.

3. For evaluation of criticality safety in the MPC-68 cask, evaluate the effects with either more accurate fresh fuel compositions (i.e., including burnable absorbers) or appropriate spent fuel compositions.

4. For scenario 5, repeat analyses for GBC-32 cask.

5. For evaluation of dose rates, evaluate the effect of greater fuel rubble compaction.

6. For evaluation of dose rates due to fuel rubble, evaluate the effect of including the axial-burnup distribution and relocation of fuel end hardware.

7. If deemed plausible, for evaluation of dose rates due to fuel rubble, evaluate the effect of fuel rubble collecting in the top/bottom of cask (beyond the "normal" active fuel position).

6 REFERENCES

1. *Standard Review Plan for Dry Cask Storage Systems*, NUREG-1536, U.S. Nuclear Regulatory Commission, Washington, D.C., January 1997.
2. *Standard Review Plan for Transportation Packages for Spent Nuclear Fuel – Final Report*, NUREG-1617, U.S. Nuclear Regulatory Commission, Washington, D.C., March 2000.
3. HI-STAR Technical Safety Analysis Report, Report HI-941184, Rev. 8, Holtec International, 1998.
4. J. C. Wagner, *Computational Benchmark for Estimation of Reactivity Margin from Fission Products and Minor Actinides in PWR Burnup Credit*, NUREG/CR-6747 (ORNL/TM-2000/306), U.S. Nuclear Regulatory Commission, Oak Ridge National Laboratory, October 2001.
5. *SCALE: A Modular Code System for Performing Standardized Computer Analyses for Licensing Evaluation*, NUREG/CR-0200, Rev. 6 (ORNL/NUREG/CSD-2/R6), Vols. I, II, III, May 2000. Available from Radiation Safety Information Computational Center at Oak Ridge National Laboratory as CCC-545.
6. S. M. Bowman and L. C. Leal, "ORIGEN-ARP: Automatic Rapid Process for Spent Fuel Depletion, Decay, and Source Term Analysis," Vol. I, Sect. D1 of *SCALE: A Modular Code System for Performing Standardized Computer Analyses for Licensing Evaluation*, NUREG/CR-0200, Rev. 6 (ORNL/NUREG/CSD-2/R6), Vols. I, II, and III, May 2000. Available from Radiation Safety Information Computational Center at Oak Ridge National Laboratory as CCC-545.
7. O. W. Hermann and C. V. Parks, "SAS2H: A Coupled One-Dimensional Depletion and Shielding Analysis Module," Vol. I, Sect. S2 of *SCALE: A Modular Code System for Performing Standardized Computer Analyses for Licensing Evaluations*, NUREG/CR-0200, Rev. 6 (ORNL/NUREG/CSD-2/R6), Vols. I, II, III, May 2000. Available from Radiation Safety Information Computational Center at Oak Ridge National Laboratory as CCC-545.
8. W. C. Jordan and S. M. Bowman, "SCALE Cross-Section Libraries," Vol. III, Sect. M4 of *SCALE: A Modular Code System for Performing Standardized Computer Analyses for Licensing Evaluations*, NUREG/CR-0200, Rev. 6 (ORNL/NUREG/CSD-2/R6), Vols. I, II, and III, May 2000. Available from Radiation Safety Information Computational Center at Oak Ridge National Laboratory as CCC-545.
9. B. L. Broadhead, *Recommendations for Shielding Evaluations for Transport and Storage Packages*, NUREG/CR-6802 (ORNL/TM-2002/31), U.S. Nuclear Regulatory Commission, Oak Ridge National Laboratory, May 2003.
10. J. S. Tang and M. B. Emmett, "SAS4: A Monte Carlo Cask Shielding Analysis Module Using An Automated Biasing Procedure," Vol. I, Sect. S4 of *SCALE: A Modular Code System for Performing Standardized Computer Analyses for Licensing Evaluations*, NUREG/CR-0200, Rev. 6 (ORNL/NUREG/CSD-2/R6), Vols. I, II, and III, May 2000. Available from Radiation Safety Information Computational Center at Oak Ridge National Laboratory as CCC-545.
11. J. T. West, T. J. Hoffman, and M. B. Emmett, "MORSE-SGC for the SCALE System," Vol. II, Sect. F9 of *SCALE: A Modular Code System for Performing Standardized Computer Analyses for Licensing Evaluations*, NUREG/CR-0200, Rev. 6 (ORNL/NUREG/CSD-2/R6), Vols. I, II, and III, May 2000. Available from Radiation Safety Information Computational Center at Oak Ridge National Laboratory as CCC-545.

12. B. L. Broadhead, M. D. DeHart, J. C. Ryman, J. S. Tang, and C. V. Parks, *Investigation of Nuclide Importance to Functional Requirements Related to Transport and Long-Term Storage of LWR Spent Fuel*, ORNL/TM-12742, Lockheed Martin Energy Systems, Inc., Oak Ridge National Laboratory, June 1995.

13. I. C. Gauld and J. C. Ryman, *Nuclide Importance to Criticality Safety, Decay Heating, and Source Terms Related to Transport and Interim Storage of High-Burnup LWR Fuel*, NUREG/CR-6700 (ORNL/TM-2000/284), U.S. Nuclear Regulatory Commission, Oak Ridge National Laboratory, January 2001.

NRC FORM 335 (2-89) NRCM 1102 3201, 3202

U.S. NUCLEAR REGULATORY COMMISSION

BIBLIOGRAPHIC DATA SHEET

(See instructions on the reverse)

1. REPORT NUMBER (Assigned by NRC, Add Vol., Supp., Rev., and Addendum Numbers, if any.)
NUREG/CR-6835
ORNL/TM-2002/255

2. TITLE AND SUBTITLE
Effects of Fuel Failure on Criticality Safety and Radiation Dose for Spent Fuel Casks

3. DATE REPORT PUBLISHED

MONTH	YEAR
September	2003

4. FIN OR GRANT NUMBER
B0009

5. AUTHOR(S)
K. R. Elam, J. C. Wagner and C. V. Parks

6. TYPE OF REPORT
Technical

7. PERIOD COVERED *(Inclusive Dates)*

8. PERFORMING ORGANIZATION — NAME AND ADDRESS *(If NRC, provide Division, Office or Region, U.S. Nuclear Regulatory Commission, and mailing address; if contractor, provide name and mailing address.)*
Oak Ridge National Laboratory, Managed by UT-Battelle, LLC
PO Box 2008, Bldg. 6700, MS-6170
Oak Ridge, TN 37831-6170

9. SPONSORING ORGANIZATION — NAME AND ADDRESS *(If NRC, type "Same as above"; if contractor, provide NRC Division, Office or Region, U.S. Regulatory Commission, and mailing address.)*
Spent Fuel Project Office
Office of Nuclear Material Safety and Safeguards
U.S. Nuclear Regulatory Commission
Washington, DC 20555-0001

10. SUPPLEMENTARY NOTES
C. J. Withee, NRC Project Manager

11. ABSTRACT *(200 words or less)*

Irradiation of nuclear fuel to high-burnup values increases the potential for fuel failure during normal and accident conditions involving transport and storage. The objective of this work is to investigate the consequences of potential fuel failure on criticality safety and external dose rates for spent nuclear fuel (SNF) storage and transport casks, with emphasis on high-burnup SNF. Analyses were performed to assess the impact of several damaged/failed fuel scenarios on the effective neutron multiplication factor (k_{eff}) and external dose rates. The damage or failure was assumed to occur during use in storage or transport, particularly in an accident. Although several of the scenarios go beyond credible conditions, they represent a theoretical limit on the effects of severe accident conditions. Further, the results provide a basis for decision making with regard to failure potential and a foundation to direct future investigations in this area.

12. KEY WORDS/DESCRIPTORS *(List words or phrases that will assist researchers in locating the report.)*
spent fuel cask, storage, transportation, criticality, shielding

13. AVAILABILITY STATEMENT
Unlimited

14. SECURITY CLASSIFICATION
(This Page) Unclassified
(This Report) Unclassified

15. NUMBER OF PAGES

16. PRICE

NRC FORM 335 (2-89)

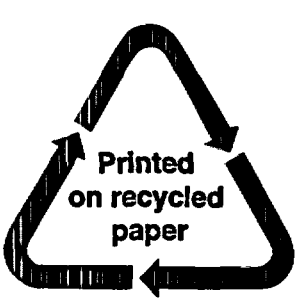

Federal Recycling Program

UNITED STATES
NUCLEAR REGULATORY COMMISSION
WASHINGTON, DC 20555-0001

OFFICIAL BUSINESS